Theory of the lattice Boltzmann method: Three-dimensional model for linear viscoelastic fluids

Pierre Lallemand,[1,*] Dominique d'Humières,[2,†] Li-Shi Luo,[3,‡] and Robert Rubinstein[4,§]
[1]*Laboratoire CNRS-ASCI, Université Paris–Sud (Paris XI Orsay), Bâtiment 506, 91405 Orsay Cedex, France*
[2]*Laboratoire de Physique Statistique de l'École Normale Supérieure, 24 Rue Lhomond, 75321 Paris Cedex 05, France*
[3]*ICASE, MS 132C, NASA Langley Research Center, Building 1152, 3 West Reid Street, Hampton, Virginia 23681-2199*
[4]*Computational Modeling and Simulation Branch, MS 128, NASA Langley Research Center, Hampton, Virginia 23681*
(Received 26 October 2000; revised manuscript received 1 October 2002; published 19 February 2003)

A three-dimensional lattice Boltzmann model with thirty two discrete velocity distribution functions for viscoelastic fluid is presented in this work. The model is based upon the generalized lattice Boltzmann equation constructed in moment space. The nonlinear equilibria of the model have a number of coupling constants that are free parameters. The dispersion equation of the model is analyzed under various conditions to obtain the constraints on the free parameters such that the model satisfies isotropy and Galilean invariance. The macroscopic equations are also derived from the lattice Boltzmann model through the dispersion equation analysis and the Chapman-Enskog analysis. We demonstrate that the dispersion equation analysis can be used as a general and effective means to derive hydrodynamic equations, excluding some nonlinear source terms, from the lattice Boltzmann model, to obtain conditions for its isotropy and Galilean invariance, and to optimize its stability. We show that the hydrodynamic behavior of the lattice Boltzmann model has memory effects, and that in the linear regime, it behaves as a viscoelastic fluid described by the Jeffreys model. Some numerical results to verify the theoretical analysis of the model are also presented.

DOI: 10.1103/PhysRevE.67.021203 PACS number(s): 83.60.Bc, 83.85.Pt, 05.20.Dd

I. INTRODUCTION

More than a decade ago, the lattice Boltzmann equation (LBE) [1–9] was introduced as a generalization of the lattice gas automata [10–12] intended as a new and possibly efficient alternative method to simulate fluid flows on parallel computers. The general principle of the lattice Boltzmann equation is to consider particles moving synchronously along the links of a highly symmetric lattice, and the dynamics of the system is fully discrete. The evolution of the LBE system at each discrete time step includes two parts: displacements and some modeled collisions that lead to a redistribution of particle populations according to some rules. The state of the system is defined by the values of the particle populations at each lattice node. In a way, this amounts to replacing the usual single-particle distribution $f(\boldsymbol{r},\boldsymbol{\xi},t)$ considered in the continuous Boltzmann equation of statistical mechanics by the set $\{f_\alpha(\boldsymbol{r}_j,t_n)|\alpha=0,1,2,\ldots,(N-1)\}$, where N is the number of discrete velocities. The quantity $f_\alpha(\boldsymbol{r}_j,t_n) \equiv f(\boldsymbol{r}_j,\boldsymbol{\xi}_\alpha,t_n)$ is the single-particle distribution function of discrete velocity $\boldsymbol{\xi}_\alpha$, on a lattice space $\boldsymbol{r}_j$, and at discrete time t_n. The lattice space $\boldsymbol{r}_j=j_1\boldsymbol{l}_1+j_2\boldsymbol{l}_2+j_3\boldsymbol{l}_3$ is represented by integer coordinates (j_1,j_2,j_3), and the basis vectors $\boldsymbol{l}_1$, $\boldsymbol{l}_2$, and $\boldsymbol{l}_3$; and discrete time $t_n=n\delta_t$, where $n\in\{0,1,\ldots\}$ and δ_t is the time step size.

To define an LBE model, several key elements need to be specified: (1) the lattice space and a set of discrete velocities, and (2) the collision rules for the redistribution of fictitious ''particles.'' The collision rules are designed to mimic the interparticle interactions in a real fluid. Once the system is specified, standard techniques in kinetic theory and statistical mechanics, such as Chapman-Enskog analysis, can be applied to derive macroscopic equations for the quantities that are slow in temporal scale and gradual in spatial scale, relative to the elemental time step δ_t and the lattice constant of the lattice space δ_x, respectively, that is, in the hydrodynamic regime. With desirable physical properties incorporated, the LBE models can be designed to simulate various simple as well as complex fluids.

The goal of the present work is to construct a three-dimensional LBE model for viscoelastic fluids. The precise microscopic mechanisms that lead to non-Newtonian behavior in real fluids are still not fully understood, but there exist many phenomenological models that mimic these fluids. The general idea in those phenomenological models is that molecules of the fluid either organize at small scale (structural relaxation) or have internal degrees of freedom, which can be affected by the local state of the fluid (due to stress, for instance). Here we shall consider the paradigm of molecular reorientation in which distortions of angular distribution functions can relax to uniform distribution.

The essential physics of viscoelasticity in non-Newtonian fluids is the interplay between hydrodynamics and the local relaxation dynamics due to internal degrees of freedom of fluid particles. Although the exact microscopic mechanisms of this interplay may be unknown, it would not prevent us from constructing a model that possesses adequate *large scale* properties of non-Newtonian fluids. We only require that the relaxation time scales due to internal degrees of freedom of fluid particles are comparable to hydrodynamic time scales, and that there exist coupling constants between macroscopic and internal degrees of freedom that can be adjusted to set the values of hydrodynamic quantities (propagation speed of various excitations and transport coefficients)

*Electronic address: lalleman@asci.fr
†Electronic address: dominiq.dhumieres@lps.ens.fr
‡Present Address: National Institute of Aerospace, 144 Research Drive, Hampton, VA 23666; Electronic address: luo@NIAnet.org; URL: http//research.NIAnet.org/~luo
§Electronic address: r.rubinstein@larc.nasa.gov

needed in the definition of nondimensional parameters (e.g., Reynolds number Re and Deborah number De, etc.) considered in numerical simulations by using the model according to the similarity principle of hydrodynamics.

The LBE model presented here is an extension of the generalized lattice Boltzmann equation by d'Humières [13] and a two-dimensional LBE model for viscoelastic fluids [14,15]. To construct a three-dimensional LBE model for athermal viscoelastic fluids, we incorporate a symmetric traceless stress tensor to mimic the effect due to internal degrees of freedom of fluid particles. The stress-tensor-like quasiconserved quantities in the model have the same symmetry as the viscous stress tensor and couple other ''fast'' kinetic modes to hydrodynamics (viscous stress tensor) [16]. We demonstrate that the LBE model presented here can simulate viscoelastic fluids described by Jeffreys model [17]. Although the proposed model is similar to an earlier two-dimensional LBE model for viscoelastic fluids [14,15], the method to analyze the LBE model is entirely different. While most previous work relies on the Chapman-Enskog analysis to obtain the hydrodynamic equations from the LBE models [14,15], we analyze the dispersion equation of the model to derive the hydrodynamic equations [18]. The analysis of the dispersion equation of the LBE system enables us to optimize the isotropy of transport coefficients. It also allows us to improve the linear stability of the model, which is beyond the capability of the standard Chapman-Enskog analysis [18] as the unstable modes have very short wavelengths.

The paper is organized as follows. Section II describes the three-dimensional LBE model for viscoelastic fluids and presents the model with linear equilibria in moment space [18]. Section III considers the dispersion equation of the linearized collision operator, and obtains the hydrodynamic modes in both low- and high-frequency limits. Transport coefficients (wave speeds and attenuation coefficients of waves) are obtained as the roots of the linearized dispersion equation. Various conditions between coupling coefficients and relaxation parameters in the model are derived by enforcing isotropy of the transport coefficients. The theoretical results of the transport coefficients are verified numerically. Section IV extends the model to include nonlinear terms in the equilibria and derives the conditions under which the model is Galilean invariant. Section V explicitly derives the macroscopic (hydrodynamic) equations of the LBE model. The model can simulate Jeffreys as well as Maxwell model of viscoelastic fluids. Finally, Sec. VII indicates possible extensions of the model and summarizes the present work. We also include two appendixes to provide a summary of all the adjustable coefficients in the model (Appendix A) needed to perform a computer simulation and the transport coefficients of the model (Appendix B).

II. THREE-DIMENSIONAL VISCOELASTIC LBE MODEL

We consider the specific case of a real viscoelastic fluid made of nonspherical particles or molecules. The state of these particles can be distorted in various ways. First, their angular distribution can be distorted when subjected to an applied stress. (If the optical properties of particles are anisotropic, then such fluids can exhibit the phenomenon of flow birefringence.) The corresponding anisotropic angular distortion can relax towards an equilibrium of isotropic distribution with a relaxation time τ, and this relaxation gives rise to a (complex) frequency-dependent shear viscosity for a periodic flow with frequency ω:

$$\nu = \nu_\infty + \frac{(\nu_0 - \nu_\infty)}{(1 + i\omega\tau)}, \tag{1}$$

where ν_0 and ν_∞ are the viscosities at the limits of $\omega \to 0$ and $\omega \to \infty$, respectively. From here on, zero- or low-frequency limit means the evolution time scales are slow relative to the relaxation time of the system, whereas ∞ or high-frequency limit means the evolution time scales are fast relative to the relaxation time of the system. Second, in addition to the angular distortion, the particles can also be stretched or compressed like a little spring. This ''elongational'' type of distortion will not be considered here as it would require taking into account internal degrees of freedom with symmetry different from what is discussed here. The effects on fluid properties due to the presence of the angular distortion are the subject of the present work.

A. Brief description of the model

As in other lattice Boltzmann models, we are going to greatly simplify the description of molecular motions of real fluids. We shall reduce the phase space available to particles. The lattice space used here is a simple three-dimensional cubic lattice space. In the following analysis, we shall use normalizations such that the lattice constant δ_x and the time step size δ_t are set to be unity, so that quantities involving spatial and temporal scales become dimensionless.

The discrete velocity set $\{\boldsymbol{e}_\alpha\}$ is chosen as the following:

$$\boldsymbol{e}_\alpha = \begin{cases} (0,0,0), & \alpha = 0 \\ (\pm 1,\pm 1,0),\ (0,\pm 1,\pm 1),\ (\pm 1,0,\pm 1), & \alpha = 1\text{–}12 \\ (\pm 1,\pm 1,\pm 1), & \alpha = 13\text{–}20 \\ (\pm 2,0,0),\ (0,\pm 2,0),\ (0,0,\pm 2), & \alpha = 21\text{–}26. \end{cases} \tag{2}$$

The discrete velocity $\boldsymbol{e}_\alpha$ is in the unit of $c = \delta_x/\delta_t = 1$. The set of the above 27 discrete velocities is the minimal one to obtain the required viscoelastic fluid properties. It should be noted that the velocities of speed 2 are chosen instead of that of speed 1 in the standard 27-velocity LBE model because of some symmetry constraints, which are discussed in the following analysis.

In order to model the angular distortion of particles, a symmetric traceless second-order stress tensor is introduced in the LBE model. This tensor in three-dimensional space can be represented by a set of five numbers:

$$(f_{27}, f_{28}, f_{29}, f_{30}, f_{31}) \equiv (m^*_{xx}, m_{ww}, m_{xy}, m_{yz}, m_{zx}), \tag{3a}$$

$$\boldsymbol{e}_\alpha = (0,0,0), \quad \alpha = 27\text{–}31, \tag{3b}$$

which are considered as five additional distribution functions of zero particle velocity, and thus do not propagate. The stress tensor specified by $\{m_{xx}^*, \ldots, m_{zx}\}$ models the anisotropic effects due to the internal degrees of freedom of particles, which are responsible for viscoelastic behaviors of a non-Newtonian fluid. Note that the traceless constraint breaks the symmetry of the diagonal elements of the tensor, this is the reason why we have introduced the element $m_{ww}=(m_{yy}-m_{zz})$, such that $m_{yy}=(m_{ww}-m_{xx})/2$ and $m_{zz}=-(m_{ww}+m_{xx})/2$, where $m_{xx}=m_{xx}^*/3$ and the factor 3 originates from the projections chosen in Eqs. (17h) and (17o). In what follows, we shall use the subscript ww to denote the difference between the last two diagonal elements.

The state of the model is therefore specified at each node of the lattice, $\boldsymbol{r}_j$, and at time $t=n$, by a set of 32 distribution functions:

$$|f(\boldsymbol{r}_j,n)\rangle \equiv (f_0(\boldsymbol{r}_j,n), f_1(\boldsymbol{r}_j,n), \ldots, f_{31}(\boldsymbol{r}_j,n))^{\mathsf{T}}, \quad (4)$$

where T is the transpose operator. From here on the Dirac notations of bra, $|\cdot\rangle$, and ket, $\langle\cdot|$, vectors are used to denoted column and row vectors, respectively.

The evolution equation of the LBE model can be written in general as the following:

$$|f(\boldsymbol{r}_j+\boldsymbol{e}_\alpha,n+1)\rangle = |f(\boldsymbol{r}_j,n)\rangle + |\Omega(f(\boldsymbol{r}_j,n))\rangle, \quad (5)$$

where Ω is the collision operator to be discussed later, and

$$|f(\boldsymbol{r}+\boldsymbol{e}_\alpha,n+1)\rangle \equiv (f_0(\boldsymbol{r}+\boldsymbol{e}_0,n+1), f_1(\boldsymbol{r}+\boldsymbol{e}_1,n+1), \ldots, f_{31}(\boldsymbol{r}+\boldsymbol{e}_{31},n+1))^{\mathsf{T}}. \quad (6)$$

Note that $\boldsymbol{e}_\alpha=\boldsymbol{0}$ for $\alpha=0$, and 27–31. Equation (5) describes both the advection due to the motions of the particles and the redistribution of the populations due to collisions.

B. Mapping between the velocity and moment space

From N distribution functions, $\{f_\alpha|\alpha=0,1,\ldots,(N-1)\}$, an equal number of moments, $\{\varrho_\alpha|\alpha=1,2,\ldots,N\}$, can be constructed without gaining or losing any information. However, the moments do have clear physical significance in the context of hydrodynamics, because they can be chosen as physical observables such as density, momentum, energy, stress, fluxes, etc. For this reason, moment space $\mathbb{M}\subset\mathbb{R}^N$ is chosen instead of the discrete velocity space $\mathbb{V}\subset\mathbb{R}^N$ to construct the LBE model, following the idea of the generalized lattice Boltzmann equation due to d'Humières [13]. The LBE model constructed in moment space $\mathbb{M}$ includes a number of adjustable parameters, the values of these parameters are varied to optimize the physical properties of the model [18]. As it has been shown [18], moment representation of the lattice Boltzmann equation is better suited to model various collision mechanisms, whereas discrete-velocity representation is natural for the advection process—a key feature of the lattice Boltzmann equation reminiscent of spectral techniques used in CFD.

We first define the basis of moment space $\mathbb{M}$, and the *linear* transformation matrix M that uniquely maps a vector $|f\rangle$ in discrete velocity space $\mathbb{V}\subset\mathbb{R}^{32}$ to a vector $|\varrho\rangle$ in moment space $\mathbb{M}\subset\mathbb{R}^{32}$, i.e.,

$$|\varrho\rangle=\mathsf{M}|f\rangle, \quad |f\rangle=\mathsf{M}^{-1}|\varrho\rangle. \quad (7)$$

For the sake of simplicity, we shall divide $\mathbb{V}$ into four subspaces according to particle speed, and first consider the mapping between each subspace of $\mathbb{V}$ and the corresponding subspace of $\mathbb{M}$.

Particles with zero velocity have only one single moment of the mass density $\rho^{(0)}$. Therefore, the mapping between the subspace $\mathbb{V}_0\subset\mathbb{R}$ and the subspace $\mathbb{M}_0\subset\mathbb{R}$ is an identity matrix of rank 1, i.e., $\mathsf{M}^{(0)}=\mathsf{I}=1$.

For the next group of 12 particles with speed $\sqrt{2}$ in the velocity subspace $\mathbb{V}_1=\mathbb{R}^{12}$, we consider the matrix

$$\mathsf{M}^{(1)}=\begin{pmatrix}
1 & 1 & 1 & 1 & 1 & 1 & 1 & 1 & 1 & 1 & 1 & 1\\
1 & -1 & 1 & -1 & 0 & 0 & 0 & 0 & 1 & 1 & -1 & -1\\
1 & 1 & -1 & -1 & 1 & -1 & 1 & -1 & 0 & 0 & 0 & 0\\
0 & 0 & 0 & 0 & 1 & 1 & -1 & -1 & 1 & -1 & 1 & -1\\
1 & 1 & 1 & 1 & -2 & -2 & -2 & -2 & 1 & 1 & 1 & 1\\
1 & 1 & 1 & 1 & 0 & 0 & 0 & 0 & -1 & -1 & -1 & -1\\
1 & -1 & -1 & 1 & 0 & 0 & 0 & 0 & 0 & 0 & 0 & 0\\
0 & 0 & 0 & 0 & 1 & -1 & -1 & 1 & 0 & 0 & 0 & 0\\
0 & 0 & 0 & 0 & 0 & 0 & 0 & 0 & 1 & -1 & -1 & 1\\
-1 & 1 & -1 & 1 & 0 & 0 & 0 & 0 & 1 & 1 & -1 & -1\\
1 & 1 & -1 & -1 & -1 & 1 & -1 & 1 & 0 & 0 & 0 & 0\\
0 & 0 & 0 & 0 & 1 & 1 & -1 & -1 & -1 & 1 & -1 & 1
\end{pmatrix}. \quad (8)$$

A vector in the subspace $\mathbf{V}_1$,

$$|\Phi^{(1)}\rangle \equiv (f_1, \ldots, f_{12})^{\mathsf{T}}, \tag{9}$$

is mapped to a vector in the corresponding subspace $\mathbb{M}_1$ of $\mathbb{M}$,

$$|\Psi^{(1)}\rangle = \mathsf{M}^{(1)}|\Phi^{(1)}\rangle = (\rho^{(1)}, j_x^{(1)}, j_y^{(1)}, j_z^{(1)}, p_{xx}^{(1)}, p_{ww}^{(1)}, p_{xy}^{(1)}, p_{yz}^{(1)}, p_{zx}^{(1)}, q_x^{(1)}, q_y^{(1)}, q_z^{(1)})^{\mathsf{T}}, \tag{10}$$

where $\rho^{(1)}$ is the mass density; $j_x^{(1)}$, $j_y^{(1)}$, $j_z^{(1)}$ are three components of the momentum (mass flux); $p_{xx}^{(1)}/3$, $(3p_{ww}^{(1)} - p_{xx}^{(1)})/6$, $-(3p_{ww}^{(1)} + p_{xx}^{(1)})/6$, $p_{xy}^{(1)}$, $p_{yz}^{(1)}$, and $p_{zx}^{(1)}$ are the components of a symmetric traceless stress tensor; and $q_x^{(1)}$, $q_y^{(1)}$, $q_z^{(1)}$ are three third-order moments (with the dimension of a flux of energy).

Similarly, for the eight distribution functions in $\mathbb{V}_2$ for the particles with speed $\sqrt{3}$, the following matrix:

$$\mathsf{M}^{(2)} = \begin{pmatrix} 1 & 1 & 1 & 1 & 1 & 1 & 1 & 1 \\ 1 & -1 & 1 & -1 & 1 & -1 & 1 & -1 \\ 1 & 1 & -1 & -1 & 1 & 1 & -1 & -1 \\ 1 & 1 & 1 & 1 & -1 & -1 & -1 & -1 \\ 1 & -1 & -1 & 1 & 1 & -1 & -1 & 1 \\ 1 & 1 & -1 & -1 & -1 & -1 & 1 & 1 \\ 1 & -1 & 1 & -1 & -1 & 1 & -1 & 1 \\ 1 & -1 & -1 & 1 & -1 & 1 & 1 & -1 \end{pmatrix} \tag{11}$$

transforms

$$|\Phi^{(2)}\rangle \equiv (f_{13}, f_{14}, \ldots, f_{20})^{\mathsf{T}} \tag{12}$$

into

$$|\Psi^{(2)}\rangle = \mathsf{M}^{(2)}|\Phi^{(2)}\rangle = (\rho^{(2)}, j_x^{(2)}, j_y^{(2)}, j_z^{(2)}, p_{xy}^{(2)}, p_{yz}^{(2)}, p_{zx}^{(2)}, q^{(2)})^{\mathsf{T}}, \tag{13}$$

where $q^{(2)}$ is a third-order moment $[\propto \Sigma_\alpha \boldsymbol{e}_{\alpha,x}\boldsymbol{e}_{\alpha,y}\boldsymbol{e}_{\alpha,z} f_\alpha]$.

Finally for six distribution functions in $\mathbb{V}_3$ for the particles with speed 2, we have the transformation matrix

$$\mathsf{M}^{(3)} = \begin{pmatrix} 1 & 1 & 1 & 1 & 1 & 1 \\ 2 & -2 & 0 & 0 & 0 & 0 \\ 0 & 0 & 2 & -2 & 0 & 0 \\ 0 & 0 & 0 & 0 & 2 & -2 \\ 8 & 8 & -4 & -4 & -4 & -4 \\ 0 & 0 & 4 & 4 & -4 & -4 \end{pmatrix}, \tag{14}$$

which transforms

$$|\Phi^{(3)}\rangle \equiv (f_{21}, f_{22}, \ldots, f_{26})^{\mathsf{T}} \tag{15}$$

to

$$|\Psi^{(3)}\rangle = \mathsf{M}^{(3)}|\Phi^{(3)}\rangle = (\rho^{(3)}, j_x^{(3)}, j_y^{(3)}, j_z^{(3)}, p_{xx}^{(3)}, p_{ww}^{(3)})^{\mathsf{T}}. \tag{16}$$

There still remain five additional distributions, $f_{27}, \ldots, f_{31}$, to be considered later. So far, only some diagonal blocks of the transform matrix M are explicitly given as $\mathsf{M}^{(0)}$, $\mathsf{M}^{(1)}$, $\mathsf{M}^{(2)}$, and $\mathsf{M}^{(3)}$. The remaining elements of M shall be given when all the moments $\{\varrho_\alpha\}$ are explicitly constructed in terms of $\{f_\alpha\}$.

According to the symmetry classes of the model, the following 32 *orthogonal* moments can be constructed from $\{f_\alpha\}$

$$\rho = \varrho_1 = \rho^{(0)} + \rho^{(1)} + \rho^{(2)} + \rho^{(3)}, \tag{17a}$$

$$e = \varrho_2 = -8\rho^{(0)} - 2\rho^{(1)} + \rho^{(2)} + 4\rho^{(3)}, \tag{17b}$$

$$\varepsilon_1 = \varrho_3 = \rho^{(1)} - 3\rho^{(2)} + 2\rho^{(3)}, \tag{17c}$$

$$\varepsilon_2 = \varrho_4 = 6\rho^{(0)} - \rho^{(1)} + \rho^{(3)}, \tag{17d}$$

$$j_{x,y,z} = \varrho_{5,8,11} = j_{x,y,z}^{(1)} + j_{x,y,z}^{(2)} + j_{x,y,z}^{(3)}, \tag{17e}$$

$$q_{x,y,z} = \varrho_{6,9,12} = -j_{x,y,z}^{(1)} + j_{x,y,z}^{(3)}, \tag{17f}$$

$$h_{x,y,z} = \varrho_{7,10,13} = j_{x,y,z}^{(1)} - 2j_{x,y,z}^{(2)} + j_{x,y,z}^{(3)}, \tag{17g}$$

$$p_{xx} = \varrho_{14} = p_{xx}^{(1)} + p_{xx}^{(3)} + cm_{xx}^*, \tag{17h}$$

$$\epsilon_{xx,ww} = \varrho_{15,17} = -2p_{xx,ww}^{(1)} + \frac{1}{4}p_{xx,ww}^{(3)}, \tag{17i}$$

$$p_{ww} = \varrho_{16} = p_{ww}^{(1)} + p_{ww}^{(3)} + bm_{ww}, \tag{17j}$$

$$p_{xy,yz,zx} = \varrho_{18,20,22} = p_{xy,yz,zx}^{(1)} + p_{xy,yz,zx}^{(2)} + am_{xy,yz,zx}, \tag{17k}$$

$$\epsilon_{xy,yz,zx} = \varrho_{19,21,23} = -2p_{xy,yz,zx}^{(1)} + p_{xy,yz,zx}^{(2)}, \tag{17l}$$

$$\eta_{x,y,z} = \varrho_{24,25,26} = q_{x,y,z}^{(1)}, \tag{17m}$$

$$h_0 = \varrho_{27} = q^{(2)}, \tag{17n}$$

$$\pi_{xx} = \varrho_{28} = -c[p_{xx}^{(1)} + p_{xx}^{(3)}] + 216m_{xx}^*, \tag{17o}$$

$$\pi_{ww} = \varrho_{29} = -b[p_{ww}^{(1)} + p_{ww}^{(3)}] + 72m_{ww}, \tag{17p}$$

$$\pi_{xy,yz,zx} = \varrho_{30,31,32} = -a[p_{xy,yz,zx}^{(1)} + p_{xy,yz,zx}^{(2)}] + 12m_{xy,yz,zx} \tag{17q}$$

where ρ is the total mass density (zeroth-order moment); e is the energy density (second-order moment); ε_1 and ε_2 are

energy square densities (fourth-order moment); $\boldsymbol{j} \equiv (j_x, j_y, j_z)$ is the mass flux or momentum density (first-order moment); $\boldsymbol{q} \equiv (q_x, q_y, q_z)$, and $\boldsymbol{\eta} \equiv (\eta_x, \eta_y, \eta_z)$ are energy fluxes (third-order moment); $\boldsymbol{h} \equiv (h_x, h_y, h_z)$ and H_0 are fluxes of energy square (fifth-order moment); $p_{xx}, \ldots, p_{zx}$ and $\pi_{xx}, \ldots, \pi_{zx}$ are second-order moments that are related to the components of two second-rank symmetric traceless stress tensors; and $\epsilon_{xx}, \ldots, \epsilon_{zx}$ are fourth-order moments that are related to the components of a symmetric and traceless second-rank tensor (products of energy and stress tensors). Three parameters, a, b, and c, are introduced to play an important role in the new physics mimicked by the LBE model coupling the hydrodynamic stress to the stress due to the internal degrees of freedom of particles. Equations (17) fully prescribe all 32 moments $\{\varrho_\alpha\}$ in terms of 32 distribution functions $\{f_\alpha\}$, and thus fully specify the transformation matrix M and its inverse M^{-1}. One may note that both M and M^{-1} involve a small number of coefficients so that the transformation from distributions to moments and *vice versa* can be efficiently accomplished in the spirit of FFT used in spectral techniques in CFD.

It should be noted that the moments given in Eqs. (17) are orthogonal, but they are not normalized. That is, for each column vector $|\varrho_\beta\rangle$ and row vector $\langle\varrho_\alpha|$ (which is a transpose of $|\varrho_\alpha\rangle$, and vice versa), we have the following orthogonal relationship:

$$\langle \varrho_\alpha | \varrho_\beta \rangle = \langle \varrho_\alpha | \varrho_\alpha \rangle \delta_{\alpha\beta}, \tag{18}$$

where $\delta_{\alpha\beta}$ is the Kronecker delta.

There are two hydrodynamic stress tensors, the components of which are either $\{p_{ij}\}$ or $\{\pi_{ij}\}$, which are coupled to the stress tensor of $\{m_{ij}\}$ due to the internal degree of freedom. The stress tensor of $\{p_{ij}\}$ simulates quasiconserved modes, whereas that of $\{\pi_{ij}\}$ mimics fast kinetic modes. The basic physics of viscoelasticity is cast in these stress tensors.

C. Equilibrium and dynamics of the model

The choice of the collision operator Ω is rather arbitrary, provided basic principles of physics are satisfied (conservation of mass and momentum, etc.). However, this arbitrariness of Ω can be reduced by considering the linearized lattice Boltzmann equation [2].

To uniquely define the operator Ω, we proceed to characterize the collision processes as linear relaxations such that the moments relax towards an equilibrium state according to simple relaxation equations with *constant* relaxation rates, and the equilibrium state depends upon the values of some of the moments. It would be natural to assume that the equilibrium state depends solely upon the conserved quantities—the mass density and the components of the momentum (mass flux) here. The equation of energy conservation is not considered here. This would lead to the following (linear) equilibrium distribution functions in general:

$$\varrho_\alpha^{(\mathrm{eq})} = \frac{1}{\langle \varrho_\alpha | \varrho_\alpha \rangle} \sum_\gamma{}' \langle \varrho_\gamma | \varrho_\gamma \rangle c_{\alpha\gamma} \varrho_\gamma, \tag{19}$$

where $c_{\alpha\gamma}$ is the coupling coefficient between ϱ_α and ϱ_γ, and the summation Σ' includes only the conserved modes, and possibly quasiconserved modes. Specifically, we have

$$e^{(\mathrm{eq})} = \frac{1}{8} a_2 \rho, \tag{20a}$$

$$\varepsilon_1^{(\mathrm{eq})} = \frac{1}{4} a_3 \rho, \tag{20b}$$

$$\varepsilon_2^{(\mathrm{eq})} = \frac{1}{2} a_4 \rho, \tag{20c}$$

$$\boldsymbol{q}^{(\mathrm{eq})} = \frac{3}{2} c_1 \boldsymbol{j}, \tag{20d}$$

$$\boldsymbol{h}^{(\mathrm{eq})} = \frac{1}{2} c_2 \boldsymbol{j}, \tag{20e}$$

where a_2, a_3, a_4, c_1, and c_2 are coupling coefficients. To allow more flexibility in the model for later analysis, we introduce an additional coupling coefficient r:

$$\epsilon_{xx}^{(\mathrm{eq})} = \frac{9A^2}{32B}(r^2 - 1) p_{xx}, \tag{21a}$$

$$\epsilon_{ww}^{(\mathrm{eq})} = \frac{9A^2}{32B}(r^2 - 1) p_{ww}, \tag{21b}$$

where

$$A = \frac{1}{(12 + a^2)}, \quad B = \frac{1}{(72 + b^2)}. \tag{22}$$

In Eqs. (21) defining ϵ_{xx} and ϵ_{ww}, the isotropy is assumed, which implies the relation between coupling coefficients a, b, and c obtained later [see Eqs. (46) in Sec. III C]. All the equilibria of the moments other than those given in Eqs. (20) and (21) should then be set to zero at linear level. Obviously, the equilibria prescribed by Eqs. (20) and (21) are not the most general ones, given the degree of freedom of the model. However, the linear equilibria capture the dominant behaviors of the model, and the nonlinear terms will be considered later in Sec. IV.

The relaxation equations of the moments are

$$\varrho_\alpha^* = \varrho_\alpha - s_\alpha [\varrho_\alpha - \varrho_\alpha^{(\mathrm{eq})}], \tag{23}$$

where s_α is the relaxation rate for the moment (or mode) ϱ_α. Decomposing the moments into equilibrium and fluctuation

$$|\varrho\rangle = |\varrho^{(\mathrm{eq})}\rangle + |\delta\varrho\rangle, \tag{24}$$

the effect of the collision step can be expressed as

$$|\varrho^*\rangle = |\varrho\rangle + \mathsf{C}|\delta\varrho\rangle, \tag{25}$$

where C is the linearized collision operator. The matrix C is mostly diagonal, with the following diagonal elements:

$$(0,-s_2,-s_3,-s_4,0,-s_6,-s_7,0,-s_6,-s_7,0,-s_6,-s_7,$$
$$-s_r,-s_{15},-s_r,-s_{15},-s_r,-s_{19},-s_r,-s_{19},-s_r,-s_{19},$$
$$-s_{24},-s_{24},-s_{24},-s_{27},-s_{28},-s_{28},-s_{30},-s_{30},-s_{30}),$$

where the symmetries of the lattice space (or obvious isotropy) have been taken into account. Among the diagonal elements of C, the four zeros correspond to four conserved quantities (ρ, j_x, j_y, and j_z). Note that the relaxation rate s_r for five components of the stress tensor, $\{p_{ij}\}$, is not necessary large (meaning close to 2 in the LBE analysis). The off-diagonal elements of C are given by

$$\langle \varrho_\alpha|\mathsf{C}|\varrho_\gamma\rangle = \frac{\langle \varrho_\gamma|\varrho_\gamma\rangle}{\langle \varrho_\alpha|\varrho_\alpha\rangle} c_{\alpha\gamma} s_\gamma. \tag{26}$$

The nonzero off-diagonal elements of C in moment space $\mathbb{M}$ are

$$\langle \rho|\mathsf{C}|e\rangle = \frac{1}{8} a_2 s_2, \tag{27a}$$

$$\langle \rho|\mathsf{C}|\varepsilon_1\rangle = \frac{1}{4} a_3 s_3, \tag{27b}$$

$$\langle \rho|\mathsf{C}|\varepsilon_2\rangle = \frac{1}{2} a_4 s_4, \tag{27c}$$

$$\langle j_i|\mathsf{C}|q_i\rangle = \frac{3}{2} c_1 s_6, \tag{27d}$$

$$\langle j_i|\mathsf{C}|h_i\rangle = \frac{1}{2} c_2 s_7, \tag{27e}$$

$$\langle \epsilon_{xx}|\mathsf{C}|p_{xx}\rangle = \frac{9A^2}{32B}(r^2-1) s_{15}, \tag{27f}$$

$$\langle \epsilon_{ww}|\mathsf{C}|p_{ww}\rangle = \frac{9A^2}{32B}(r^2-1) s_{15}. \tag{27g}$$

In velocity space $\mathbb{V}$, Eq. (25) becomes

$$|f^*\rangle = |f\rangle + \mathsf{M}^{-1}\mathsf{C}\mathsf{M}|\delta f\rangle. \tag{28}$$

III. DISPERSION EQUATION AND HYDRODYNAMIC MODES

There are two approaches to deriving the hydrodynamic behavior of the model: (1) the Chapman-Enskog analysis, modified for the situation of some moderate relaxation rates, to derive macroscopic equations directly from the model [14,15]; and (2) analysis of dispersion equations of the model [18]. Although the Chapman-Enskog procedure is the conventional means most often used in the LBE analysis, we shall use the analysis of dispersion equation in the present work to study the hydrodynamic behavior of the LBE model.

A. Dispersion equation and its eigenvalue problem

We study the behavior of the system subject to an initial condition that is the superposition of a uniform equilibrium state and a small spatially periodic fluctuation with wave vector $\boldsymbol{k}$, such that $k \ll 1$:

$$f_\alpha(\boldsymbol{r}_j,t) = f_\alpha^{(0)} + \phi_\alpha(\boldsymbol{r}_j,t), \tag{29}$$

where $f_\alpha^{(0)}$ is a spatially uniform and steady equilibrium and $\phi_\alpha(\boldsymbol{r}_j,t)$ is the fluctuation. The wavelength of the fluctuation is large compared to the lattice spacing δ_x $(=1)$. We solve the linearized dispersion equation to obtain the solutions of the form $\exp(i\boldsymbol{k}\cdot\boldsymbol{r}+st)$ corresponding to the hydrodynamic modes of the system.

Fourier transform in $\boldsymbol{r}_j$ of the linearized evolution equation of ϕ_α gives [19,20]

$$\mathsf{A}|\phi(\boldsymbol{k},t+1)\rangle = |\phi(\boldsymbol{k},t)\rangle + \mathsf{M}^{-1}\mathsf{C}\mathsf{M}|\phi(\boldsymbol{k},t)\rangle, \tag{30}$$

where advection operator A is a diagonal matrix:

$$\mathsf{A}_{\alpha\beta} = \exp(i\boldsymbol{e}_\alpha\cdot\boldsymbol{k})\,\delta_{\alpha\beta}. \tag{31}$$

Therefore,

$$|\phi(\boldsymbol{k},t+1)\rangle = \mathsf{H}|\phi(\boldsymbol{k},t)\rangle, \tag{32}$$

where the evolution operator

$$\mathsf{H} \equiv \mathsf{A}^{-1}[\mathsf{I} + \mathsf{M}^{-1}\mathsf{C}\mathsf{M}]. \tag{33}$$

The eigenvalue problem of H provides the generalized hydrodynamics of the system, i.e., for an eigenvalue λ_α of H,

$$\gamma_\alpha = \ln \lambda_\alpha \tag{34}$$

allows us to determine wave number dependent phase velocity and transport coefficient of the system.

Laplace transform of Eq. (30) in time leads to the following dispersion equation:

$$\det[\mathsf{A}e^s - \mathsf{I} - \mathsf{M}^{-1}\mathsf{C}\mathsf{M}] = 0. \tag{35}$$

Usually the dispersion equation cannot be solved analytically. For small k and s, we expand A and e^s in Taylor series in $\boldsymbol{k}$ and s, respectively:

$$\mathsf{A}_{\alpha\beta} = \mathsf{I} + \mathsf{K}^{(1)} + \mathsf{K}^{(2)} + \cdots, \tag{36a}$$

$$\mathsf{K}^{(n)}_{\alpha\beta} = \frac{1}{n!}(i\boldsymbol{e}_\alpha\cdot\boldsymbol{k})^n \delta_{\alpha\beta}, \tag{36b}$$

and consider the dispersion equation linear in $\boldsymbol{k}$ and s,

$$\det[\mathsf{M}\mathsf{K}^{(1)}\mathsf{M}^{-1}-\mathsf{C}+s\mathsf{I}]=0. \tag{37}$$

Note that the linearized dispersion equation in effect has only included first-order spatial and temporal derivatives because it is only first order in both $\boldsymbol{k}$ and s. As was first demonstrated by Hénon in his analysis of the lattice gas automata [21], second-order derivatives due to the presence of the lattice should be included in the analysis. It is understood that the effect of the corresponding second-order derivatives amounts to a correction of the terms $1/s_\alpha$ by $(1/s_\alpha-1/2)$. Therefore, for the sake of simplicity, we can omit second-order derivatives in the analysis for now and make the correction later simply by replacing $1/s_\alpha$ by $(1/s_\alpha-1/2)$. We shall use the following substitution whenever it is appropriate:

$$\frac{1}{\tilde{s}_\alpha}\equiv\frac{1}{s_\alpha}-\frac{1}{2}. \tag{38}$$

The linearized dispersion equation (37) is a polynomial of degree 32 in s and $\boldsymbol{k}=(k_x,k_y,k_z)$. Because it is difficult to compute the roots of the dispersion equation analytically, even by perturbation technique in the limit of $k\to 0$, further approximation must be made in order to solve Eq. (37). We note that in contrast with four conserved quantities, all other nonconserved quantities relax towards their equilibria with constant relaxation rates $\{s_\alpha\}$. Therefore, we can consider $1/\tilde{s}_\alpha>0$ as small parameters, and solve the linearized dispersion equation correct to the order of $1/\tilde{s}_\alpha$ under two circumstances. First, assuming that $k\ll\tilde{s}_\alpha$ including $\tilde{s}_r$, Gaussian elimination can be used to reduce the size of the determinant from 32×32 to 4×4 for four hydrodynamic modes (two transverse and two longitudinal modes). This leads to ''low-frequency'' modes. In effect, all the kinetic modes (modes other than the conserved ones) are treated as ''fast modes'' and have to be eliminated.

The second approximation considered is that $k\ll\tilde{s}_\alpha$ except $\tilde{s}_r$. In this case, the size of the determinant reduces to 9×9 involving five components of the stress tensor $\{p_{ij}\}$ in addition to four conserved quantities. The four conserved quantities as well as five quasiconserved quantities, $\{p_{ij}\}$, are separated from the remaining 23 ''fast'' modes. In this case, the nine modes are the ''high-frequency modes.'' The values of propagating speeds and attenuation rates of various waves are obtained by solving the dispersion equation. Note that from now on, ''low'' and ''high'' frequencies are defined with respect to s_r, and that we are in the low-frequency regime with respect to the 23 fast modes of the system.

B. Low-frequency modes

The reduced form of the dispersion equation to a 4×4 determinant allows us to find two longitudinal modes with phase velocity

$$c_s=\frac{1}{12}\sqrt{2(62+a_2)}, \tag{39}$$

and two transverse modes that relax exponentially with a rate $\gamma_T^0 k^2$. The isotropy of γ_T^0 implies that the five relaxation rates for the moments $\{p_{ij}\}$ are equal (s_r), and furthermore that

$$\tilde{s}_{28}=\frac{b^2}{6a^2}\tilde{s}_{30}. \tag{40}$$

Under such conditions, we have

$$\gamma_T^0=c_T^2\left[\left(\frac{1}{s_r}-\frac{1}{2}\right)+\frac{a^2}{12}\left(\frac{1}{s_{30}}-\frac{1}{2}\right)\right], \tag{41a}$$

$$c_T^2=\frac{3}{2}\frac{(4-3c_1-c_2)}{(12+a^2)}. \tag{41b}$$

Longitudinal waves have an amplitude that relaxes exponentially with an equivalent damping constant related to

$$\gamma_L^0=\frac{1}{2}\left(\zeta_0+\frac{4}{3}\gamma_T^0\right), \tag{42}$$

$$\zeta_0=\left(1+\frac{1}{2}c_1-c_s^2\right)\left(\frac{1}{s_2}-\frac{1}{2}\right)=\frac{1}{72}(8+36c_1-a_2)\left(\frac{1}{s_2}-\frac{1}{2}\right), \tag{43}$$

where ζ_0 is the bulk viscosity. Note at this stage that a simplified analysis involving but one relaxation rate in the LBE model, i.e., the lattice Bhatnagar-Gross-Krook (LBGK) model [3,4,22,23,28], could not lead to an isotropic behavior unless the particular choice of $b=a\sqrt{6}$ (i.e., $s_{28}=s_{30}$) is made. (It should be noted that two-dimensional LBE models in Refs. [22,23] for viscoelastic fluids may not be extended to three-dimensional space when isotropy and Galilean invariance are considered for minimally damped transverse waves.)

C. High-frequency modes

We now consider larger values of k so that $k\ll\tilde{s}_r$ no longer holds, but $k\ll\tilde{s}_\alpha$ and $\tilde{s}_\alpha\gg\tilde{s}_r$. As indicated above, the application of Gaussian elimination reduces the 32×32 determinant in Eq. (35) to a 9×9 determinant involving five components of the stress tensor $\{p_{ij}\}$, in addition to four conserved quantities (one ρ and three components of $\boldsymbol{j}$).

The reduced dispersion equation up to the order of $\boldsymbol{k}$, with 9×9 determinant, is

$$\begin{vmatrix}
s & ik_x & ik_y & ik_z & 0 & 0 & 0 & 0 & 0 \\
ic_s^2k_x & s & 0 & 0 & i24Bk_x & 0 & i12Ak_y & 0 & i12Ak_z \\
ic_s^2k_y & 0 & s & 0 & -i12Bk_y & i36Bk_y & i12Ak_x & i12Ak_z & 0 \\
ic_s^2k_z & 0 & 0 & s & -i12Bk_z & -i36Bk_z & 0 & i12Ak_y & i12Ak_x \\
0 & i2\kappa_1k_x & -i\kappa_1k_y & -i\kappa_1k_z & s+\tilde{s}_r & 0 & 0 & 0 & 0 \\
0 & 0 & i\kappa_1k_y & -i\kappa_1k_z & 0 & s+\tilde{s}_r & 0 & 0 & 0 \\
0 & i\kappa_2k_y & i\kappa_2k_x & 0 & 0 & 0 & s+\tilde{s}_r & 0 & 0 \\
0 & 0 & i\kappa_2k_z & i\kappa_2k_y & 0 & 0 & 0 & s+\tilde{s}_r & 0 \\
0 & i\kappa_2k_z & 0 & i\kappa_2k_x & 0 & 0 & 0 & 0 & s+\tilde{s}_r
\end{vmatrix} = 0, \tag{44}$$

where

$$\kappa_1 = \frac{3}{8}(4+7c_1+c_2), \tag{45a}$$

$$\kappa_2 = \frac{1}{8}(4-3c_1-c_2), \tag{45b}$$

and A and B are given by Eq. (22). With $\tilde{s}_r$ substituted in Eq. (44) for s_r, some k^2 terms have been included implicitly in the analysis. The wave vector can be written in spherical coordinates,

$$\boldsymbol{k} = (k_x, k_y, k_z) = k(\cos\phi \sin\theta, \sin\phi \sin\theta, \cos\theta).$$

We are seeking solutions such that $s = ivk$. The propagating behavior of the model will be isotropic if the wave speed v is independent of the orientation of $\boldsymbol{k}$, i.e., θ and ϕ.

If we assume $\tilde{s}_r \neq 0$, then the leading term in k in the dispersion equation (44) is of the order k^4. Setting the leading term to zero leads to the following solutions: $v = 0$ for two diffusive modes (nonpropagating modes), and $v = \pm c_s$ for two low-frequency acoustic modes.

If we assume $\tilde{s}_r = 0$, the leading term is now of the order k^9. The solution for the wave speed can be made isotropic if we choose

$$c = \sqrt{3}b, \tag{46a}$$

$$B = \frac{(4-3c_1-c_2)}{9(4+7c_1+c_2)}A. \tag{46b}$$

With the above choices of c and B, the dispersion equation (44) has two pairs of roots with opposite speeds $v = \pm c_T$, and one pair of roots with opposite speeds $v = \pm c_L$, where

$$c_T^2 = \frac{3}{2}(4-3c_1-c_2)A, \tag{47a}$$

$$c_L^2 = \frac{4}{3}c_T^2 + c_s^2. \tag{47b}$$

In addition, there are two roots with propagating speed $v = 0$, which shall be referred to as nonpropagating or diffusive modes. The above relation of Eq. (47b) between propagating speeds of transverse and longitudinal waves is precisely what is expected in a viscoelastic fluid [24].

Note that the determinant in the dispersion equation (44) can be simplified if $\boldsymbol{k}$ is along one of the axes (e.g., x axis). This can be accomplished by applying a rotational transformation to the determinant. If wave vector $\boldsymbol{k}$ is rotated to align with x axis, and if c and B satisfy Eqs. (46), then in the rotated space, dispersion equation (44) becomes

$$\begin{vmatrix}
s & ik & 0 & 0 & 0 & 0 & 0 & 0 & 0 \\
ic_s^2k & s & \frac{3}{2}ic_T^2k & 0 & 0 & 0 & 0 & 0 & 0 \\
0 & \frac{8}{9}ik & s+\tilde{s}_r & 0 & 0 & 0 & 0 & 0 & 0 \\
0 & 0 & 0 & s & ic_T^2k & 0 & 0 & 0 & 0 \\
0 & 0 & 0 & ik & s+\tilde{s}_r & 0 & 0 & 0 & 0 \\
0 & 0 & 0 & 0 & 0 & s & ic_T^2k & 0 & 0 \\
0 & 0 & 0 & 0 & 0 & ik & s+\tilde{s}_r & 0 & 0 \\
0 & 0 & 0 & 0 & 0 & 0 & 0 & s+\tilde{s}_r & 0 \\
0 & 0 & 0 & 0 & 0 & 0 & 0 & 0 & s+\tilde{s}_r
\end{vmatrix} = 0. \tag{48}$$

In the above determinant, there are five irreducible diagonal blocks. The first 3×3 block, coupling ρ, j_x, and P_{xx}, has one pair of longitudinal modes propagating with wave speed $\pm c_L$ and one diffusive (nonpropagating) longitudinal mode; the next two 2×2 blocks, coupling j_y and P_{xy} (or j_z and P_{xz}), represent two pairs of transverse modes propagating with wave speed $\pm c_T$; and the last two 1×1 blocks represent two diffusive stress modes, corresponding to the stress components P_{ww} and P_{yz}.

Analysis of the 2×2 blocks in Eq. (48) shows that the transverse modes are propagative (wave) modes for wave numbers larger than the critical wave number k_c, defined by

$$\frac{1}{k_c}=2c_T\left(\frac{1}{s_r}-\frac{1}{2}\right), \tag{49}$$

and that the attenuation of waves is related to a relaxing shear viscosity as in Eq. (1). The dependence of the critical wave number on the relaxation parameter s_r, which affects transverse waves [see Eq. (41a)] is one of the key features of the model for viscoelastic fluids.

At low-frequency limit $k\ll\tilde{s}_r$, the results [of c_T and c_L given by Eqs. (47)] obtained here reduce to that of the preceding section [the solution for c_s of Eq. (39)]. At high frequency, the contributions from higher-order moments (beyond the stress tensor) become significant.

In order to analyze the attenuation of the waves, i.e., to obtain solution as $s=iuk-\gamma k^2$, k^2 terms must be included in the dispersion determinant in the expansion of $\boldsymbol{k}$, i.e., the dispersion equation must include $\mathsf{K}^{(2)}$ as the following:

$$\det[\mathsf{M}(\mathsf{K}^{(1)}+\mathsf{K}^{(2)})\mathsf{M}^{-1}-\mathsf{C}+s\mathsf{I}]=0. \tag{50}$$

The analysis of the above equation becomes rather tedious algebraically, even though it is a 9×9 determinant. We shall therefore only outline the analysis, and provide the final results in the following.

We first consider the infinite frequency limit, i.e., $\tilde{s}_r=0$. The attenuation of the transverse modes is obtained from the coefficient of k^{11} of the expansion of Eq. (50) in powers of k. The attenuation is highly anisotropic, strongly dependent on the orientation of $\boldsymbol{k}$, i.e. on θ and ϕ, for arbitrary values of the parameters in the model. However, this anisotropy can be eliminated by the following choice of relaxation parameters in addition to Eq. (40):

$$\tilde{s}_6=\omega_6\tilde{s}_{27}, \tag{51a}$$

$$\tilde{s}_7=\omega_7\tilde{s}_{27}, \tag{51b}$$

$$\tilde{s}_{24}=\frac{1}{4}\tilde{s}_{27}, \tag{51c}$$

and ω_6 and ω_7 are complicated functions of r, c_1, and c_2 (see details in Appendix A).

The attenuation of the longitudinal modes still depends on the orientation of $\boldsymbol{k}$ even when the preceding conditions of Eqs. (51) are satisfied. This angular dependence of the longitudinal attenuation is obtained by setting the angular dependence of the coefficient of k^{10} to zero. It can actually be eliminated by introducing a relationship between the parameters a_3 and a_4 (see further discussions in Sec. V C and details in Appendix A).

Finally, the relaxation of the two nonpropagating stress modes can be considered. These modes relax exponentially with a rate $-D_0k^2$ (diffusive behavior). The diffusivity D_0 is anisotropic (angle dependent) unless some relationships among c_1, c_2, and r are satisfied (see Appendix A). When these relationships are taken into account, we have

$$D_0=\frac{8}{(12+a^2)}\left(\frac{1}{s_{27}}-\frac{1}{2}\right). \tag{52}$$

D. Isotropic criteria of the model

The requirement for isotropy will depend upon the definition of isotropy. If we limit the isotropy to that of the damping of the propagating modes, then a simpler model than the present one would achieve the goal (only 26 moments are needed in that case; no particle with speed 2 are needed). If we demand the diffusive stress modes to be isotropic as well, then we need the present 32 moment model in which a specific relationship between c_1, c_2, and r must be satisfied. If in addition we want longitudinal and transverse modes to be decoupled up to second order in $\boldsymbol{k}$, then we have to choose a particular value of either c_1 or c_2. The results given in Appendix A are obtained based on the most stringent conditions considered here, i.e., the wave speeds and attenuation rates of propagating modes and attenuation of diffusive modes are all isotropic.

IV. NONLINEAR ANALYSIS AND GALILEAN INVARIANCE

A. Nonlinear equilibria and Galilean invariance

One of the difficulties encountered in the lattice gas automata was the lack of Galilean invariance, leading to nonlinear advection terms different from that in the Navier-Stokes equations [10–12]. With a set of bounded discrete velocities, neither the lattice gas automata nor the lattice Boltzmann equation can satisfy Galilean invariance rigorously. That is, both the lattice gas automata and the lattice Boltzmann equation are inherently non-Galilean invariant [25]. Nevertheless, the defect due to the non-Galilean invariance can be systematically improved (order by order in $\boldsymbol{k}$) by increasing the number of discrete velocities. Inclusion of a large enough set of discrete velocities in the lattice Boltzmann equation allows one to solve that difficulty in practice.

The approach we shall use here considers the effect of a mean uniform flow with a mean velocity $\boldsymbol{V}$ superimposed to small amplitude fluctuations. Galilean invariance of the system means that the speed of various waves with wave vector $\boldsymbol{k}$ shall be $u(0)+\boldsymbol{V}\cdot\hat{\boldsymbol{k}}$, where $u(0)$ is the wave speed at $\boldsymbol{V}=\boldsymbol{0}$, and $\hat{\boldsymbol{k}}\equiv\boldsymbol{k}/k$.

With the assumption that $V \gg |\phi_\alpha|$, we shall repeat the analysis performed in the linear dispersion equation. However, in order to correctly consider the effect due to the mean flow velocity $\boldsymbol{V}$, the equilibria of various moments must include nonlinear terms. We consider the following general nonlinear equilibria, of which the linear part remains intact [i.e., the same as Eqs. (20) and (21)]:

$$\varrho_\alpha^{(\mathrm{eq})} = \sum_\gamma{}' \frac{\langle \varrho_\gamma | \varrho_\gamma \rangle}{\langle \varrho_\alpha | \varrho_\alpha \rangle} c_{\alpha\gamma} \varrho_\gamma + \sum_{\gamma,\mu}{}' \frac{\langle \varrho_\gamma | \varrho_\gamma \rangle \langle \varrho_\mu | \varrho_\mu \rangle}{\langle \varrho_\alpha | \varrho_\alpha \rangle \langle \varrho_\alpha | \varrho_\alpha \rangle} c_{\alpha\gamma\mu} \varrho_\gamma \varrho_\mu, \tag{53}$$

where $c_{\alpha\gamma\mu}$ is the second-order coupling coefficient. Obviously, the most general consideration of $\varrho_\alpha^{(\mathrm{eq})}$ would include a large number of coupling constants so that analytic treatment of the problem becomes too laborious. To reduce the number of coupling constants we only include the terms that satisfy symmetry considerations and dimensional analysis. We propose to use the following second-order equilibria,

$$e^{(\mathrm{eq})} = \frac{1}{8} a_2 \rho + 3 \frac{\boldsymbol{j}\cdot\boldsymbol{j}}{\rho}, \tag{54a}$$

$$\boldsymbol{q}^{(\mathrm{eq})} = \frac{3}{2} c_1 \boldsymbol{j} + A_1 \frac{\boldsymbol{j}\cdot\mathsf{p}}{\rho} + A_2 \frac{\boldsymbol{j}\cdot\mathsf{d}}{\rho}, \tag{54b}$$

$$\boldsymbol{h}^{(\mathrm{eq})} = \frac{1}{2} c_2 \boldsymbol{j} + A_3 \frac{\boldsymbol{j}\cdot\mathsf{p}}{\rho} + A_4 \frac{\boldsymbol{j}\cdot\mathsf{d}}{\rho}, \tag{54c}$$

$$p_{xx}^{(\mathrm{eq})} = A_5 \frac{2j_x^2 - j_y^2 - j_z^2}{\rho}, \tag{54d}$$

$$p_{ww}^{(\mathrm{eq})} = A_5 \frac{j_y^2 - j_z^2}{\rho}, \tag{54e}$$

$$p_{il}^{(\mathrm{eq})} = A_6 \frac{j_i j_l}{\rho}, \quad i \neq l, \quad i, \quad l \in \{x,y,z\}, \tag{54f}$$

$$\pi_{xx}^{(\mathrm{eq})} = A_7 \frac{2j_x^2 - j_y^2 - j_z^2}{\rho}, \tag{54g}$$

$$\pi_{ww}^{(\mathrm{eq})} = A_8 \frac{j_y^2 - j_z^2}{\rho}, \tag{54h}$$

$$\pi_{il}^{(\mathrm{eq})} = A_9 \frac{j_i j_l}{\rho}, \quad i \neq l, \quad i, \quad l \in \{x,y,z\}, \tag{54i}$$

$$\eta_x^{(\mathrm{eq})} = -\frac{j_x(p_{yy} - p_{zz})}{3\rho} - 2\frac{j_y p_{xy} - j_z p_{xz}}{\rho}, \tag{54j}$$

$$\eta_y^{(\mathrm{eq})} = -\frac{j_y(p_{zz} - p_{xx})}{3\rho} - 2\frac{j_z p_{yz} - j_x p_{xy}}{\rho}, \tag{54k}$$

$$\eta_z^{(\mathrm{eq})} = -\frac{j_z(p_{xx} - p_{yy})}{3\rho} - 2\frac{j_x p_{xz} - j_y p_{yz}}{\rho}, \tag{54l}$$

$$h_0^{(\mathrm{eq})} = \frac{j_x p_{yz} + j_y p_{xz} + j_z p_{xy}}{\rho}, \tag{54m}$$

$$\epsilon_{ii}^{(\mathrm{eq})} = \frac{9A^2}{32B}(r^2 - 1) p_{ii},, \quad i \in \{x,w\}, \tag{54n}$$

where the second-rank tensors p and d are given by

$$p_{yy} \equiv (3p_{ww} - p_{xx})/2, \tag{55a}$$

$$p_{zz} \equiv -(p_{xx} + p_{yy}), \tag{55b}$$

$$\mathsf{p}_{il} \equiv p_{il}, \quad i, \quad l \in \{x,y,z\}, \tag{55c}$$

$$\mathsf{d} \equiv \mathrm{diag}(p_{xx}, p_{yy}, p_{zz}). \tag{55d}$$

The linearized collision operator can be determined up to the first order in $\boldsymbol{V}$ as the following:

$$\mathsf{C}_{\alpha\gamma}(\boldsymbol{V}) = s_\alpha \frac{\partial \varrho_\alpha^{(\mathrm{eq})}}{\partial \varrho_\gamma} - s_\alpha \delta_{\alpha\gamma}. \tag{56}$$

The speeds of longitudinal and transverse waves at both low and high frequencies are determined through the dispersion equation of the above linearized collision operator. Our aim is to solve the dispersion equation and obtain the wave speeds behaving as $v(0) + gV\cos\vartheta$, where $v(0)$ is the wave speed when $\boldsymbol{V} = \boldsymbol{0}$ (up to the first order in V), and ϑ is the angle between $\boldsymbol{V}$ and wave vector $\boldsymbol{k}$. Galilean invariance implies that $g = 1$. Isotropy and Galilean invariance ($g = 1$) lead to

$$A_1 = \frac{1}{3}\left[\frac{(A+9B)}{B}\frac{c_T^2}{c_s^2} - 9\right], \tag{57a}$$

$$A_2 = \frac{1}{3}\left[\frac{2(A+9B)}{A}\frac{c_T^2}{c_s^2} - 3\right] - A_1, \tag{57b}$$

$$A_3 = \frac{1}{3}\left[9 - \frac{(A+21B)}{B}\frac{c_T^2}{c_s^2}\right], \tag{57c}$$

$$A_4 = \frac{1}{3}\left[9 - \frac{2(A+21B)}{A}\frac{c_T^2}{c_s^2}\right] - A_3, \tag{57d}$$

$$A_5 = \frac{1}{72B}\frac{c_T^2}{c_s^2}, \tag{57e}$$

$$A_6 = \frac{1}{12A}\frac{c_T^2}{c_s^2}, \tag{57f}$$

$$A_7 = \frac{3}{Bc}\left(\frac{c_T^2}{c_s^2} - 1\right), \tag{57g}$$

$$A_8=\frac{1}{Bb}\left(\frac{c_T^2}{c_s^2}-1\right), \tag{57h}$$

$$A_9=\frac{1}{Aa}\left(\frac{c_T^2}{c_s^2}-1\right). \tag{57i}$$

With the equilibria determined, we can show that the model is indeed Galilean invariant in the $\boldsymbol{k}=\boldsymbol{0}$ limit, at both low and high frequencies:

$$g_T^0=1, \quad g_L^0=1, \tag{58a}$$

$$g_T^\infty=1, \quad g_L^\infty=1. \tag{58b}$$

B. Dispersion equation linear in V

With the linearized collision operator determined up to the first order in $\boldsymbol{V}$ according to Eq. (56) with the nonlinear equilibria given by Eqs. (54), the dispersion equation also depends on $\boldsymbol{V}$, and so are the roots of the dispersion equation, which determine the speeds and attenuation rates of various waves.

The dispersion equation with linear equilibria is independent of $\boldsymbol{V}$, and is given by Eq. (44) up to first order in $\boldsymbol{k}$. In the rotated coordinate system such that wave vector $\boldsymbol{k}$ is along with one of the axes, Eq. (44) becomes Eq. (48). The nonlinear contribution of $\mathsf{C}(\boldsymbol{V})$ to the dispersion equation is first order in $\boldsymbol{k}$ and $\boldsymbol{V}$ as well. Under the same coordinate system of Eq. (48), and if $\boldsymbol{V}$ is parallel to the wave vector $\boldsymbol{k}$ (along one of the axes), the contribution from the quadratic parts of the nonlinear equilibria to the dispersion equation, which is linear in $\boldsymbol{V}$ and $\boldsymbol{k}$, amounts to the following:

$$V\begin{vmatrix} 0 & 0 & 0 & 0 & 0 & 0 & 0 & 0 & 0 \\ 0 & ik\chi_1 & 0 & 0 & 0 & 0 & 0 & 0 & 0 \\ 0 & \frac{8\tilde{s}_r}{9c_s^2} & ik\chi_2 & 0 & 0 & 0 & 0 & 0 & 0 \\ 0 & 0 & 0 & ik\chi_3 & 0 & 0 & 0 & 0 & 0 \\ 0 & 0 & 0 & \frac{\tilde{s}_r}{c_s^2} & ik\chi_4 & 0 & 0 & 0 & 0 \\ 0 & 0 & 0 & 0 & 0 & ik\chi_3 & 0 & 0 & 0 \\ 0 & 0 & 0 & 0 & 0 & \frac{\tilde{s}_r}{c_s^2} & ik\chi_4 & 0 & 0 \\ 0 & 0 & 0 & 0 & 0 & 0 & 0 & ik & 0 \\ 0 & 0 & 0 & 0 & 0 & 0 & 0 & 0 & ik \end{vmatrix}, \tag{59}$$

where

$$\chi_1=2-\frac{4c_T^2}{3c_s^2}, \tag{60a}$$

$$\chi_2=1+\frac{4c_T^2}{3c_s^2}, \tag{60b}$$

$$\chi_3=1-\frac{c_T^2}{c_s^2}, \tag{60c}$$

$$\chi_4=1+\frac{c_T^2}{c_s^2}. \tag{60d}$$

Therefore, the determinant of (59) should be added in the left hand side of the dispersion equation (48) to consider the effect due to a finite mean flow velocity $\boldsymbol{V}$.

Our analysis on Galilean invariance can be verified by either direct numerical solution of the dispersion equation depending on $\boldsymbol{V}$ [i.e., including the determinant of (59)] or direct numerical simulation of relaxation of waves in the LBE model. The numerical results from these two methods confirm that the LBE model is indeed Galilean invariant at both low and high frequencies. We also find that the attenuation of waves depends upon $\boldsymbol{V}$, and this dependence cannot be suppressed even for a small value of k. (The analysis of $\boldsymbol{V}$ dependence of the attenuation of waves requires the dispersion equation to include terms up to second order in $\boldsymbol{k}$.) Considering models with more discrete velocities might help solve this problem.

V. MACROSCOPIC EQUATIONS

The way to proceed follows closely what has been done in the preceding section. First, to avoid typographic complications, we do not include in the following derivations second-order derivatives in space that come from the fact that the lattice Boltzmann equation is a finite difference equation on a lattice. As indicated previously, a ''Hénon correction'' at the end can be a remedy to the problem.

From Eq. (30) we have the following 32 linear equations for the fluctuation

$$\partial_t \varphi_\alpha + \sum_{\beta,\gamma} \mathsf{M}^{-1}_{\alpha\beta} \mathsf{M}_{\beta\gamma} \boldsymbol{e}_\beta \cdot \boldsymbol{\nabla} \varphi_\gamma = s_\alpha \varphi_\alpha, \tag{61}$$

where $|\varphi\rangle \equiv \mathsf{M}|\phi\rangle$ is the fluctuation of the moments. We arrange the moments in the following order. First, the four conserved quantities (density and its flux), then the five quasiconserved quantities p_{ij}, and then all other moments. The remaining 23 modes can be called ''fast'' modes, similar to the treatment of the Langevin equation in statistical mechanics. Assuming that the 23 relaxation rates are large, we can perform a successive elimination of the corresponding equations keeping only terms of order 1 and $1/\tilde{s}_\alpha$. This way to proceed leads to nine equations of motion that include up to second-order derivatives in space. We assume that we start from an initial condition where the ''fast'' modes have small amplitudes and contribute only to order $1/\tilde{s}_\alpha$, and thus will be neglected.

This process leads to cumbersome expressions. Some simplifications can be achieved using some of the results of the preceding section (relationships between *a*, *b*, and *c*, and expressions for $\tilde{s}_{28}/\tilde{s}_{30}$ and $\tilde{s}_{24}/\tilde{s}_{27}$). We shall now present the results for various orders in spatial derivatives. These results will be considered as the equation of motion of an equivalent macroscopic fluid (EMF) to be distinguished from the full LBE model.

A. Zeroth- and first-order spatial derivatives

To simplify the analysis, we first change scale for the five quasiconserved quantities that we call

$$Q_{xx} = \frac{16}{9(4+7c_1+c_2)} p_{xx}, \tag{62a}$$

$$Q_{ww} = \frac{16}{9(4+7c_1+c_2)} p_{ww}, \tag{62b}$$

$$Q_{il} = \frac{8}{4-3c_1-c_2} p_{il}, \quad i \neq l, \quad i,\ l \in \{x,y,z\}, \tag{62c}$$

and define the elements of a symmetric traceless tensor Q by

$$Q_{yy} = \frac{1}{2}(3Q_{ww} - Q_{xx}), \tag{63}$$

$$Q_{zz} = -(Q_{xx} + Q_{yy}), \tag{64}$$

$$\mathsf{Q}_{il} \equiv Q_{il}, \quad i,\ l \in \{x,y,z\}. \tag{65}$$

Collecting all terms of order 0 and 1, we get the following set of equations:

$$\partial_t \rho + \boldsymbol{\nabla} \cdot \boldsymbol{j} = 0, \tag{66a}$$

$$\partial_t \boldsymbol{j} + \boldsymbol{\nabla} \cdot \mathsf{P} = 0, \tag{66b}$$

$$\partial_t \mathsf{Q} + \hat{\mathsf{D}}^* = -s_r \mathsf{Q}, \tag{66c}$$

where $\boldsymbol{j} = \rho \boldsymbol{u}$, and

$$\mathsf{P} \equiv c_s^2 \rho \mathsf{I} + c_T^2 \mathsf{Q}, \tag{67a}$$

$$\dot{\mathsf{D}}^* \equiv (\boldsymbol{\nabla} \boldsymbol{j}) + (\boldsymbol{\nabla} \boldsymbol{j})^\dagger, \quad \hat{\mathsf{D}}^* \equiv \dot{\mathsf{D}}^* - \frac{2}{3} \mathsf{I} \boldsymbol{\nabla} \cdot \boldsymbol{j}. \tag{67b}$$

The superscript † represents the transpose operation on a second-order tensor. The above equations could be used to determine the long-wavelength modes ($k \to 0$) of the EMF. This would lead to the same conclusions as in the preceding section.

B. Second-order spatial derivatives

We shall consider successively various second-order terms (second-order spatial derivatives). The expressions that we shall write should be included on the left hand side of the previous equations of order 0 and 1. When only some of these equations are concerned, we shall indicate between parentheses which equation to modify at second order.

1. Bulk viscosity at low-frequency limit

Terms in $1/s_2$ contribute only to the mass flux equations of $\boldsymbol{j}$,

$$\boldsymbol{j}: \quad \zeta_0 \boldsymbol{\nabla} \boldsymbol{\nabla} \cdot \boldsymbol{j}, \tag{68}$$

where the bulk viscosity at low-frequency limit, ζ_0, is given by Eq. (43). The above term appears in the right hand side of the equation for $\boldsymbol{j}$ in Eqs. (66).

2. The modes associated with $\{m_{xx}, m_{ww}, m_{xy}, m_{yz}, m_{zx}\}$

These five quantities have the symmetry of a symmetric traceless second-rank tensor and contribute only to the flux equations

$$\boldsymbol{j}: \quad \tilde{\nu}_0 \left(\boldsymbol{\nabla}^2 \boldsymbol{j} + \frac{1}{3} \boldsymbol{\nabla} \boldsymbol{\nabla} \cdot \boldsymbol{j} \right), \tag{69}$$

where the nonrelaxing shear viscosity at low-frequency limit is given by

$$\tilde{\nu}_0 = \frac{1}{8}(4 - 3c_1 - c_2 - 8c_T^2) \left(\frac{1}{s_{30}} - \frac{1}{2} \right). \tag{70}$$

3. The other modes of higher order in velocity

These modes usually play no role in an ordinary fluid. They have an anisotropic contribution for the EMF unless care is taken in the choice of the parameters of the model. First, there are terms that involve the second-order derivative of the density, their expressions are

$$Q_{xx}: \quad \frac{2b_2}{3}(2\partial_{xx}^2\rho-\partial_{yy}^2\rho-\partial_{zz}^2\rho), \tag{71a}$$

$$Q_{ww}: \quad \frac{2b_2}{3}(\partial_{yy}^2\rho-\partial_{zz}^2\rho), \tag{71b}$$

$$Q_{ij}: \quad b_1\partial_{ij}^2\rho, \quad i\neq j, \quad i,j\in\{x,y,z\}, \tag{71c}$$

we shall consider them later. Second, there are terms involving Q_{ij}

$$\begin{aligned} Q_{xx}: \quad & (r_1+r_2)\nabla^2Q_{xx}+3r_2\partial_{xx}^2Q_{xx}-3r_2(\partial_{yy}^2-\partial_{zz}^2)Q_{ww} \\ & +2b_5(\partial_{xy}^2Q_{xy}-2\partial_{yz}^2Q_{yz}+\partial_{zx}^2Q_{zx}), \end{aligned} \tag{72a}$$

$$\begin{aligned} Q_{ww}: \quad & (r_1+3r_2)\nabla^2Q_{ww}-r_2(\partial_{yy}^2-\partial_{zz}^2)Q_{xx}-3r_2\partial_{xx}^2Q_{ww} \\ & +2b_5(\partial_{xy}^2Q_{xy}-\partial_{zx}^2Q_{zx}), \end{aligned} \tag{72b}$$

$$\begin{aligned} Q_{xy}: \quad & (3b_4+b_6)\nabla^2Q_{xy}-3b_3\partial_{yz}^2Q_{zz}-3b_4(\partial_{zz}^2Q_{xy} \\ & -\partial_{zx}^2Q_{yz}-\partial_{yz}^2Q_{zx}), \end{aligned} \tag{72c}$$

$$\begin{aligned} Q_{yz}: \quad & (3b_4+b_6)\nabla^2Q_{yz}-3b_3\partial_{yz}^2Q_{xx}-3b_4(\partial_{xx}^2Q_{yz} \\ & -\partial_{xy}^2Q_{zx}-\partial_{xz}^2Q_{xy}), \end{aligned} \tag{72d}$$

$$\begin{aligned} Q_{zx}: \quad & (3b_4+b_6)\nabla^2Q_{zx}-3b_3\partial_{yz}^2Q_{yy}-3b_4(\partial_{yy}^2Q_{zx} \\ & -\partial_{yz}^2Q_{xy}-\partial_{yx}^2Q_{yz}). \end{aligned} \tag{72e}$$

A number of coefficients (b_1, b_2, b_3, b_4, b_5, b_6, r_1, and r_2) introduced in Eqs. (71) and (72) are functions of r, c_1, c_2, and of s_6, s_7, and s_{27} [s_{24} has been substituted by Eq. (51c)]. Similar to the preceding section, the adjustment of parameters in the above equations can be used to enforce the isotropy of the model.

The minimal isotropy condition is obtained when the attenuation coefficients of small k excitations do not depend upon the orientation of $\boldsymbol{k}$. This can be achieved when the following relations are satisfied:

$$b_1=2(b_2+b_3-2b_4+b_5), \tag{73a}$$

$$r_1=-3b_3+6b_4-3b_5+b_6, \tag{73b}$$

$$r_2=b_3-b_4+b_5. \tag{73c}$$

Isotropy can be imposed for the nonpropagating modes. This leads to

$$b_5=2b_4-b_3, \tag{74}$$

and simplifies the previous conditions (73) to

$$b_1=2b_2, \quad r_1=b_6, \quad r_2=b_4. \tag{75}$$

Finally, longitudinal and transverse modes can be fully decoupled if

$$b_5=b_4. \tag{76}$$

When the above condition is satisfied, the corresponding equations involve a term diagonal in Q_{ij} proportional to r_1 (which is interpreted as a diffusion coefficient), a traceless symmetric tensor for Q_{ij} proportional to r_2 that we interpret as a shear viscous contribution. In addition, there is a coupling between Q_{ij} and derivatives of the density proportional to b_2, which is interpreted as a bulk viscous contribution. By substituting b_2, b_3, b_4, b_5, and b_6 in terms of r_1 and r_2 into Eqs. (72), we have

$$\begin{aligned} Q_{xx}: \quad & (r_1+r_2)\nabla^2Q_{xx}+3r_2\partial_{xx}^2Q_{xx}-3r_2(\partial_{yy}^2-\partial_{zz}^2)Q_{ww} \\ & +2r_2(\partial_{xy}^2Q_{xy}-2\partial_{yz}^2Q_{yz}+\partial_{zx}^2Q_{zx}), \end{aligned} \tag{77a}$$

$$\begin{aligned} Q_{ww}: \quad & (r_1+3r_2)\nabla^2Q_{ww}-r_2(\partial_{yy}^2-\partial_{zz}^2)Q_{xx}+2r_2(\partial_{xy}^2Q_{xy} \\ & -\partial_{xx}^2Q_{ww}-\partial_{zx}^2Q_{zx}), \end{aligned} \tag{77b}$$

$$\begin{aligned} Q_{xy}: \quad & (r_1+3r_2)\nabla^2Q_{xy}-3r_2\partial_{yz}^2Q_{zz}-3r_2(\partial_{zz}^2Q_{xy} \\ & -\partial_{zx}^2Q_{yz}-\partial_{zy}^2Q_{zx}), \end{aligned} \tag{77c}$$

$$\begin{aligned} Q_{yz}: \quad & (r_1+3r_2)\nabla^2Q_{yz}-3r_2\partial_{yz}^2Q_{xx}-3r_2(\partial_{xx}^2Q_{yz} \\ & -\partial_{xy}^2Q_{zx}-\partial_{xz}^2Q_{xy}), \end{aligned} \tag{77d}$$

$$\begin{aligned} Q_{zx}: \quad & (r_1+3r_2)\nabla^2Q_{zx}-3r_2\partial_{yz}^2Q_{yy}-3r_2(\partial_{yy}^2Q_{zx} \\ & -\partial_{yz}^2Q_{xy}-\partial_{yx}^2Q_{yz}). \end{aligned} \tag{77e}$$

When the ''full'' isotropy is satisfied, the attenuation coefficients of high-frequency modes are given by:

$$\gamma_T^\infty=\frac{1}{2}(3b_4+b_6)+\frac{1}{2}\tilde{\nu}_0, \tag{78a}$$

$$\gamma_L^\infty=\frac{2c_T^2(b_2+4b_4+b_6)}{(3c_s^2+4c_T^2)}+\frac{1}{2}\tilde{\nu}_0+\frac{2}{3}\zeta_0, \tag{78b}$$

$$\gamma_0^\infty=\frac{[3c_s^2(4b_4+b_6)-2b_1c_T^2]}{(3c_s^2+4c_T^2)}, \tag{78c}$$

$$D_0=b_6, \tag{78d}$$

where γ_0^∞ corresponds to the diffusive longitudinal mode, and the contributions to γ_T^∞ and γ_L^∞ from the moments other than the stress tensor have been included.

The question now is whether it is possible to satisfy all the relationships between the parameters indicated above. It turns out that the present model has a sufficient number of free parameters to achieve the full isotropy. The detailed expressions of the parameters are provided in Appendix A. There is still some freedom in the choice of the remaining parameters, this freedom will be used to obtain positive attenuation coefficients, positive values of ω_6, and ω_7, and to improve stability of the model for large values of k.

C. Dispersion equation up to second order in k

The preceding results regarding the attenuation coefficients of high-frequency modes can also be obtained by the analysis of the dispersion equation up to second order in $\boldsymbol{k}$. In the coordinate system where the wave vector $\boldsymbol{k}$ is along one of the axes, the following 9×9 determinant should be included in the left hand side of Eq. (48) for the ''high-frequency'' attenuation of various modes:

$$-k^2\begin{vmatrix} 0 & 0 & 0 & 0 & 0 & 0 & 0 & 0 & 0 \\ 0 & 0 & 0 & 0 & 0 & 0 & 0 & 0 & 0 \\ \frac{8}{9}b_2 & 0 & (r_1+4r_2) & 0 & 0 & 0 & 0 & 0 & 0 \\ 0 & 0 & 0 & 0 & 0 & 0 & 0 & 0 & 0 \\ 0 & 0 & 0 & 0 & (r_1+3r_2) & 0 & 0 & 0 & 0 \\ 0 & 0 & 0 & 0 & 0 & 0 & 0 & 0 & 0 \\ 0 & 0 & 0 & 0 & 0 & 0 & (r_1+3r_2) & 0 & 0 \\ 0 & 0 & 0 & 0 & 0 & 0 & 0 & r_1 & 0 \\ 0 & 0 & 0 & 0 & 0 & 0 & 0 & 0 & r_1 \end{vmatrix}, \tag{79}$$

and the ''low-frequency'' contribution to the damping of longitudinal and transverse modes in Eq. (48) is related to the following 9×9 determinant:

$$-k^2\begin{vmatrix} 0 & 0 & 0 & 0 & 0 & 0 & 0 & 0 & 0 \\ 0 & \zeta_0 & 0 & 0 & 0 & 0 & 0 & 0 & 0 \\ 0 & 0 & 0 & 0 & 0 & 0 & 0 & 0 & 0 \\ 0 & 0 & 0 & \left(\zeta_0+\frac{4}{3}\tilde{\nu}_0\right) & 0 & 0 & 0 & 0 & 0 \\ 0 & 0 & 0 & 0 & 0 & 0 & 0 & 0 & 0 \\ 0 & 0 & 0 & 0 & 0 & \left(\zeta_0+\frac{4}{3}\tilde{\nu}_0\right) & 0 & 0 & 0 \\ 0 & 0 & 0 & 0 & 0 & 0 & 0 & 0 & 0 \\ 0 & 0 & 0 & 0 & 0 & 0 & 0 & 0 & 0 \\ 0 & 0 & 0 & 0 & 0 & 0 & 0 & 0 & 0 \end{vmatrix}, \tag{80}$$

where $\tilde{\nu}_0$ and ζ_0 are the nonrelaxing shear and bulk viscosities, given by Eqs. (70) and (43), respectively. Obviously the model is isotropic up to second order in $\boldsymbol{k}$ because the dispersion equation, including Eqs. (79) and (80), is independent of the orientation of $\boldsymbol{k}$.

D. Hydrodynamic equations for equivalent macroscopic fluid

To summarize the preceding discussion, we can combine Eqs. (66), (68), (69), (71), and (77) to obtain hydrodynamic equations. This leads to the following hydrodynamic equations for the equivalent macroscopic fluid derived from the LBE model:

$$\partial_t\rho+\nabla\cdot\boldsymbol{j}=0, \tag{81a}$$

$$\partial_t\,\boldsymbol{j}+\nabla\cdot(\boldsymbol{uj})=-\nabla\cdot\mathsf{P}+\tilde{\nu}_0\nabla^2\boldsymbol{j}+\eta_0\nabla\nabla\cdot\boldsymbol{j}, \tag{81b}$$

$$\partial_t \mathsf{Q} + \boldsymbol{\nabla}\cdot(\boldsymbol{u}\mathsf{Q}) + \frac{c_T^2}{c_s^2}\left[(\boldsymbol{\nabla}\boldsymbol{u})^\dagger\cdot\mathsf{Q} + \mathsf{Q}\cdot(\boldsymbol{\nabla}\boldsymbol{u}) - \frac{2}{3}\,\mathrm{Tr}[\mathsf{Q}\cdot(\boldsymbol{\nabla}\boldsymbol{u})]\mathsf{I}\right] = -s_r\mathsf{Q} + r_1\boldsymbol{\nabla}^2\mathsf{Q} + 3r_2\mathsf{S} - \rho\hat{\mathsf{D}} + b_1\widehat{\boldsymbol{\nabla}\boldsymbol{\nabla}}\rho + \left(1-\frac{c_T^2}{c_s^2}\right)\Gamma + \left(1-\frac{A}{6B}\right)\Theta - \left(1-\frac{6B}{A}\right)\Psi, \tag{81c}$$

where $\boldsymbol{u}=\boldsymbol{j}/\rho$, $\mathsf{P}=c_s^2\rho\mathsf{I}+c_T^2\mathsf{Q}$, $\hat{\mathsf{D}}$ is the traceless part of the rate of strain tensor $\dot{\mathsf{D}}$,

$$\hat{\mathsf{D}}\equiv\dot{\mathsf{D}}-\frac{2}{3}(\boldsymbol{\nabla}\cdot\boldsymbol{u})\mathsf{I},\quad \dot{\mathsf{D}}\equiv(\boldsymbol{\nabla}\boldsymbol{u})+(\boldsymbol{\nabla}\boldsymbol{u})^\dagger \tag{82}$$

[with $(\boldsymbol{\nabla}\boldsymbol{u})_{ij}\equiv\partial_i u_j$] and other tensors are defined as follows:

$$\mathsf{S}\equiv(\boldsymbol{\nabla}\boldsymbol{\nabla}\cdot\mathsf{Q})+(\boldsymbol{\nabla}\boldsymbol{\nabla}\cdot\mathsf{Q})^\dagger-\frac{2}{3}\mathrm{Tr}(\boldsymbol{\nabla}\boldsymbol{\nabla}\cdot\mathsf{Q})\mathsf{I}, \tag{83a}$$

$$\widehat{\boldsymbol{\nabla}\boldsymbol{\nabla}}\equiv\boldsymbol{\nabla}\boldsymbol{\nabla}-\frac{1}{3}\boldsymbol{\nabla}\cdot\boldsymbol{\nabla}\mathsf{I}, \tag{83b}$$

$$\Gamma\equiv(\Omega\cdot\mathsf{Q})+(\Omega\cdot\mathsf{Q})^\dagger-(\mathsf{W}\cdot\mathsf{Q})-(\mathsf{W}\cdot\mathsf{Q})^\dagger, \tag{83c}$$

$$\Omega\equiv(\boldsymbol{\nabla}\boldsymbol{u})-(\boldsymbol{\nabla}\boldsymbol{u})^\dagger, \tag{83d}$$

$$\mathsf{W}\equiv(\boldsymbol{u}\boldsymbol{\nabla})-(\boldsymbol{u}\boldsymbol{\nabla})^\dagger \tag{83e}$$

$$\Theta\equiv(\Omega-\mathsf{W})*\Sigma, \tag{83f}$$

$$\Sigma_{ij}\equiv\mathsf{Q}_{ii}-\mathsf{Q}_{jj},\quad i,\ j\in\{x,y,z\}, \tag{83g}$$

$$\Psi\equiv\Gamma*\mathsf{I}, \tag{83h}$$

the symbol Tr indicates the trace of a tensor, and the symbol $*$ in Eq. (83f) defines the component-by-component multiplication operation between the two tensors (i.e., if $\mathsf{A}=\mathsf{B}*\mathsf{C}$, then $\mathsf{A}_{ij}=\mathsf{B}_{ij}\mathsf{C}_{ij}$). The parameters b_1, b_2, r_1, and r_2 are given in Appendix A, and

$$\eta_0=\zeta_0+\frac{1}{3}\tilde{\nu}_0 \tag{84}$$

is the bulk viscosity of the model.

Although we did not show any detailed expressions for the hydrodynamic equations previously derived using the dispersion equation and the Chapman-Enskog expansion, it has been verified that both approaches give exactly the same relationships between the model parameters. This includes the nonlinear convective terms involving products of $\boldsymbol{u}$ and $\boldsymbol{\nabla j}$ or $\boldsymbol{\nabla}\mathsf{Q}$ leading to Galilean invariance. However, the terms involving products of $\boldsymbol{j}$ or Q and $\boldsymbol{\nabla u}$ have only been obtained from the Chapman-Enskog analysis.

The nonlinear terms ensure Galilean invariance of the model when the average velocity is parallel to the wave vector. However, when the velocity is perpendicular to the wave vector, the additional terms related to Γ, Θ, and Ψ couple the different linear hydrodynamic modes in two ways: the leading mode for the mean flow motion acts as a source for the others with an amplitude linear in the average transverse velocity $\boldsymbol{V}_T$; this coupling changes the damping of the leading mode with a term quadratic in $\boldsymbol{V}_T$.

The term related to Γ could probably be removed by setting $c_s=c_T$ with no side effects other than an increased compressibility. However, the condition $A=6B$, under which the two anisotropic terms related to Θ and Ψ would disappear, cannot be enforced: this requires $r=-\frac{1}{3}$ [cf. Eq. (A4) in Appendix A], a value for which the coupling coefficient a_4 in Eq. (20c) is ill-defined [cf. Eq. (A3c) in Appendix A].

Equation (81c) has been written in a form as close as possible to the usual "convected model" [17]. Since the Jaumann derivative is the only material derivative that can be obtained for a symmetric traceless tensor, we had expected to obtain it. It turns out that instead, the left-hand side of Eq. (81c) looks very similar to the traceless version of the so-called upper-convected Maxwell derivative of Q, but with opposite sign for the term $[(\boldsymbol{\nabla}\boldsymbol{u})^\dagger\cdot\mathsf{Q}+\mathsf{Q}\cdot(\boldsymbol{\nabla}\boldsymbol{u})]$.

We have therefore achieved our goal of finding an EMF that has all the properties of linear viscoelastic fluids. If we consider the equation for one of the components of Q, we find that apart from the term proportional to a second-order differential operator, it is identical to the equation for a Jeffreys fluid. The influence of the second-order differential operator could be minimized by working under such conditions that $\tilde{s}_r \gg b_6 k^2$. This is easily achieved in a real fluid, as it is commonly observed that the ratio of microscopic to macroscopic time scales can be extremely small. However, in the LBE simulations, such separation of scale, although possible in principle, is limited by practical considerations including the number of nodes of the lattice and the duration of the simulation.

VI. NUMERICAL SOLUTION OF THE DISPERSION EQUATION AND SIMULATION OF WAVE PROPAGATION IN THE THREE-DIMENSIONAL LBE VISCOELASTIC MODEL

The results discussed in Sec. III on the dispersion equation can be verified in two ways: (1) direct computation of the roots of the full dispersion equation given by Eq. (35) without any approximation, or (2) direct numerical simulation of the LBE model and determination of how initial spatially periodic excitations relax in time. Both types of tests were conducted to verify our theoretical analysis.

For the direct numerical solution of the dispersion equation of Eq. (35), it is noted that the lattice Boltzmann equation is a finite difference equation on a regular lattice, so its solutions are of the form $z^t e^{i(k_x a_x + k_y a_y + k_z a_z)}$. As shown in the beginning of this section, the dispersion equation is equivalent to an eigenvalue problem for which efficient and accurate numerical techniques are readily available, regardless of the value of $\boldsymbol{k}$. The roots of the dispersion equation $\{z_\alpha|\,\alpha=1,\ldots,32\}$ can be computed as functions of $\boldsymbol{k}$, and $\gamma_\alpha(\boldsymbol{k})=\ln z_\alpha(\boldsymbol{k})$ is the relaxation rate for the corresponding mode $|\varrho_\alpha\rangle$. For $k\ll 1$, the numerical values of γ_α corresponding to

hydrodynamic modes (i.e., $\gamma_\alpha|_{\boldsymbol{k}=\boldsymbol{0}}=0$) are in excellent agreement with the analytical results up to second order in $\boldsymbol{k}$ (provided that the ''Hénon correction'' is adequately considered). It should be stressed that the direct eigenvalue analysis of the dispersion equation (to numerically compute z_α) is very useful for large values of k, the situation in which the usual Chapman-Enskog analysis would not work. The eigenvalue analysis also leads to further ''tuning'' of the adjustable parameters of the model in order to improve the numerical stability of the model, i.e., to avoid situations where the real part of one or more z_α becomes positive, which would obviously cause the model to be unstable.

The direct simulation of the LBE model, which is the ultimate aim of the present work, turns out to be quite simple to perform, and the LBE algorithm is rather fast on a modern workstation. It is easy to initiate either longitudinal or transverse waves of a given wave vector $\boldsymbol{k}$ in an LBE system with periodic boundary conditions. Fourier analysis of time series of density or transverse velocity fluctuations allows one to determine both phase velocities and relaxation coefficients. These quantities are found to be in excellent agreement with the previous theory for systems large enough so that dispersion effects due to the lattice discreteness can be neglected (i.e., $k \ll 1$). The relative accuracy for the phase velocities (both longitudinal and transverse) is better than 0.01% and that for the attenuation coefficients is better than 0.1%.

When k is no longer small, the results of the simulation are in good agreement with the direct numerical computation of z_α. Even for unstable situations [i.e., $\mathrm{Re}(z_\alpha)>0$ for some α], the wave vector of the observed ''diverging'' mode obtained from the direct LBE simulation is in good agreement with the one leading to largest value of the real part of $z_\alpha(\boldsymbol{k})$. As this usually occurs for large values of k, this means that the lattice Boltzmann algorithm is valid up to large values of k where its accuracy might be questionable.

The illustrate our point, we simulated wave propagation in the LBE model under various conditions. A system of size $N_x \times N_y \times N_z$ with periodic boundaries is used to test the wave propagations in the three-dimensional lattice Boltzmann model for viscoelastic fluids. The initial condition of the velocity field is a uniform velocity $\boldsymbol{V}=(V_x,V_y,V_z)$ plus a fluctuation $\delta\boldsymbol{u}$:

$$\boldsymbol{u}(\boldsymbol{x},t=0)=\boldsymbol{V}+\delta\boldsymbol{u}\cdot\cos(\boldsymbol{k}\cdot\boldsymbol{x}), \tag{85}$$

where the wave vector $\boldsymbol{k}=(k_x,k_y,k_z)$ is chosen such that the periodic boundary conditions are satisfied, i.e., $k_i=2n\pi/N_i$, for integer n and $i\in\{x,y,z\}$. As the system evolves, the spatial Fourier transform of velocity $\tilde{\boldsymbol{u}}(\boldsymbol{k},t)$ can be computed, and the transverse ($\boldsymbol{u}_T$) and longitudinal ($\boldsymbol{u}_L$) modes (with respect to $\boldsymbol{k}$) can be determined.

For the case of a zero uniform velocity $\boldsymbol{V}=(0,0,0)$, the transverse and longitudinal modes behave as follows:

$$\boldsymbol{u}_T(t)=\boldsymbol{u}_T(0)\exp(-\gamma_T k^2 t), \tag{86a}$$

$$\boldsymbol{u}_L(t)=\boldsymbol{u}_L(0)\cos(\omega t)\exp(-\gamma_L k^2 t), \tag{86b}$$

where $\omega=kc_s$ in the low-frequency region and $\omega=kc_T$ in the high-frequency region along the direction of $\boldsymbol{k}$. For a nonzero uniform velocity $\boldsymbol{V}$, the transverse components behave as

$$\boldsymbol{u}_T(t)=\boldsymbol{u}_T(0)\cos(\boldsymbol{k}\cdot\boldsymbol{V}t)\exp(-\gamma_T k^2 t), \tag{87}$$

whereas the longitudinal components behave in a more complicated fashion as the beat note of two signals oscillating at different frequencies:

$$\boldsymbol{u}_L(t)=\boldsymbol{u}_L(0)\{\cos[(\boldsymbol{k}\cdot\boldsymbol{V}+\omega)t]\pm\cos[(\boldsymbol{k}\cdot\boldsymbol{V}-\omega)t]\}\times\exp(-\gamma_L k^2 t). \tag{88}$$

The simulation of wave propagations allows us to extract information of the phase [ω and $(\boldsymbol{k}\cdot\boldsymbol{V}\pm\omega)$] and the relaxation of amplitudes (γ_T and γ_L). The results of phases and attenuation rates of the wave obtained by the direct numerical simulations agree very well with the results obtained by directly computing the roots of the dispersion equation for the same value of the wave vector (the relative error is about 0.01%).

We simulated wave propagations in the three-dimensional viscoelastic media in both low and high frequency regions, and with and without a uniform velocity of the fluid $\boldsymbol{V}$. The system size is $N_x \times N_y \times N_z = 269\times 3\times 2$. The wavevector is chosen be parallel to x axis, i.e., $\boldsymbol{k}=(k_x,0,0)$, and $k_x=4\times 2\pi/N_x$. It should be noted that this particular choice of $\boldsymbol{k}$ in the simulation does not affect the generality of the analysis. The same analysis was also applied to wave vectors parallel to (1,1,0) and (1,1,1). The value of the adjustable parameters used in the simulations are $a=3$, $a_2=-20$, $a_3=-0.13$, $r=-0.47$, $s_2=1.95$, $s_3=1.30$, $s_4=1.60$, $s_{15}=1.30$, $s_{19}=1.40$, $s_{24}=1.50$, and $s_{29}=1.90$. With the parameter values given, $c_s=\sqrt{22}/6\approx 0.7817$ and $c_T\approx 0.5723$. Figures 1 and 2 show dynamic behaviors of various waves in low-frequency and high-frequency regions, corresponding to $s_r=1.95$ and $s_r=0$, respectively, and with or without a constant mean flow velocity $\boldsymbol{V}$. It is important to note that, in the present model, the relaxation times for different waves can be adjusted individually, which is impossible for the LBGK-type models [22,23]. In particular, when $s_r=0$, the corresponding relaxation time is infinite, this certainly cannot be achieved by the LBGK-type models [22,23].

VII. DISCUSSION AND CONCLUSION

In this work we have presented a three-dimensional lattice Boltzmann model for viscoelastic fluids. By carefully analyzing the dispersion equation of the model, we can make the model isotropic and Galilean invariant. In addition, the remaining adjustable coupling coefficients in the model provide the freedom to optimize the numerical stability of the model. The proposed model is capable of simulating linear viscoelastic fluids in three dimensions and could be readily extended (by using a more complicated dynamics for the ''internal'' modes) to reproduce subtle phenomena such as the Senftleben-Beenakker effect in gases (cf. Ref. [26], Sec. 3.4), or to simulate nematic liquid crystals, and even bipolar

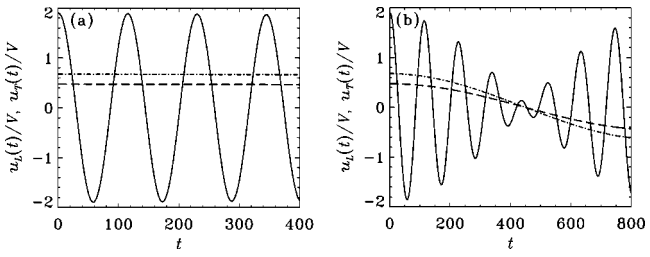

FIG. 1. Relaxation of longitudinal and transverse waves in the low-frequency regime. The values of adjustable coupling constants in the simulations are $a=3$, $a_2=-20$, $a_3=-0.13$, and $r=-0.47$, and the values of relaxation parameters are $s_2=1.95$, $s_3=1.30$, $s_4=1.60$, $s_{15}=1.30$, $s_{19}=1.40$, $s_{24}=1.50$, $s_{29}=1.90$, and $s_r=0$. The solid, dashed, and dot-dashed lines represent amplitudes of one longitudinal and two transverse waves at a particular location, respectively, normalized by $V=0.05$; (a) $\boldsymbol{V}=(0,0,0)$ and (b) $\boldsymbol{V}=(0.05,0,0)$, in lattice units ($\delta_x=\delta_t=1$).

fluids under the influence of external magnetic field.

We have also extended the analysis of dispersion equation of simple fluids [18] to complex fluids. It should be stressed that the linear dispersion equation analysis is equivalent to the Chapman-Enskog analysis in the sense that both of them derive the hydrodynamic equations from the lattice Boltzmann equation. However, the analysis of dispersion equation can also provide linear stability analysis for large wave number k, which the Chapman-Enskog analysis cannot do; whereas the Chapman-Enskog analysis can obtain some nonlinear terms that cannot be obtained by the linear dispersion equation analysis. Therefore, the dispersion equation analysis, in general, can serve as a powerful tool to study the lattice Boltzmann models complementary to the Chapman-Enskog analysis.

The model constructed in the present work simulates *athermal* viscoelastic fluids. The energy equation is not considered for the following reasons. First, only nearly incompressible fluids are considered here (therefore there are no shocks in the fluid). Second, the stability remains a difficult problem for thermal lattice Boltzmann model, partly due to a finite number of discrete velocities [25] and the linearity of the relaxation model of the LBE model considered here [27]. Third, in order to have a correct thermal conductivity, the relaxation rates s_6 and s_7 must be related (i.e., the influence of higher-order moments on the heat transfer) in a way incompatible to Eqs. (51a) and (51b). This means that the model needs additional degrees of freedom to accommodate this relationship between s_6 and s_7. Finally, through the analysis of the dispersion equation, we found that the linear stability of the model degrades as the mean flow velocity increases. This would limit the application of the present model to simulate flows with moderate Reynolds number. To resolve all these issues, it is inevitable to have a more complex model, and this is left for future study. However, it is worth to mention that one effective alternative to incorporate thermal effects in the model is to solve the energy equation independently by using finite difference or other techniques [27]. This approach completely decouples the energy equation from the mass and momentum equations and thus removes the spurious coupling between the energy and shear modes, which instigates the numerical instability in the energy-conserving LBE models [27].

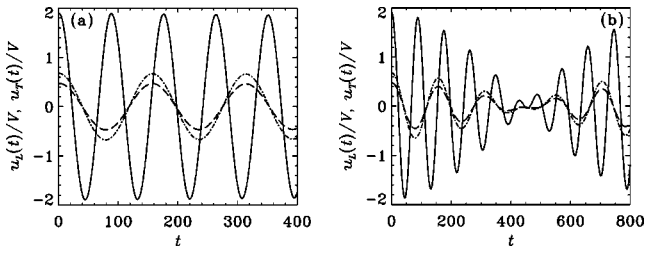

FIG. 2. Relaxation of longitudinal and transverse waves in the high-frequency regime. The values of adjustable parameters in the simulations are the same as in the simulations shown in Fig. (1), except $s_r=1.95$; (a) $\boldsymbol{V}=(0,0,0)$ and (b) $\boldsymbol{V}=(0.05,0,0)$, in lattice units ($\delta_x=\delta_t=1$).

There are several directions to extend the present model in the future. Consideration of one additional scalar quantity would introduce a frequency-dependent bulk viscosity in the model, as is done to characterize dispersion of sound. Adding a nonvanishing trace to the second-order tensor with components $\{p_{ij}\}$ could be useful to mimic ''elongational'' effects. Including more traceless tensors may be useful to reproduce nonexponential decay, as is observed in most situations in reality, with more or less complicated behavior if couplings between the internal modes are adequately considered. It becomes apparent to us that in order to have a lattice Boltzmann model to correctly simulate three-dimensional viscoelastic fluids, the model must possess certain necessary features to satisfy the proper couplings among different waves in low- and high-frequency regions, and isotropy and Galilean invariance. Our experience indicates that some existing LBE models for viscoelastic fluids in two dimensions [22,23] are unlikely to satisfy the necessary conditions and may not be easily extended to three dimensions because these models do not possess sufficient degrees of freedom to accommodate these necessary conditions.

We also realize that, although the dispersion equation analysis can be systematically applied to the LBE models in general, the analytical treatment of the dispersion equation can become intractable algebraically when the number of adjustable parameters becomes large for complex models. Therefore, it is highly desirable to minimize the number of parameters in an LBE model, and the research is under way by the authors.

ACKNOWLEDGMENTS

P.L. and D.d'H. would like to acknowledge financial support from ICASE during their visits to ICASE, and L.S.L. would like to acknowledge the financial support from CNRS for his visits to ASCI Laboratory where part of this work was done. L.S.L. would also like to acknowledge partial support from the United States Air Force Office for Scientific Research under Grant No. F49620-01-1-0142.

APPENDIX A: PARAMETERS IN THE MODEL

Among the adjustable parameters in the model, there are three coupling coefficients in stress tensors $\{p_{ij}\}$ and $\{\pi_{ij}\}$:

a, b, and c, and there are six coupling coefficients in the equilibria: a_2, a_3, a_4, c_1, c_2, and r. The isotropy of the high-frequency wave speed (c_T) leads to

$$c=\sqrt{3}b, \tag{A1a}$$

$$B=\frac{(4-3c_1-c_2)}{9(4+7c_1+c_2)}A, \tag{A1b}$$

where

$$A=\frac{1}{(12+a^2)}, \quad B=\frac{1}{(72+b^2)}. \tag{A2}$$

The isotropy of the attenuation coefficients further leads to the following relations between the coupling coefficients:

$$c_1=\frac{2(27r^3-471r^2+197r+55)}{3(21r-29)(15r^2+8r-15)}, \tag{A3a}$$

$$c_2=-2\frac{R_1}{R_2}, \tag{A3b}$$

$$R_1=(297r^3-357r^2-89r+85),$$

$$R_2=(9r-17)(15r^2+8r-15),$$

$$a_4=12+\frac{(R_3a_3-18R_4c_s^2)}{8(r-1)(21r-29)(3r+1)}, \tag{A3c}$$

$$R_3=(99r^3+201r^2-1075r+583),$$

$$R_4=(243r^3-543r^2+269r+95),$$

$$b_1=\frac{(r+3)(R_2a_3+6R_1c_s^2)}{12(r-1)R_5}\left(\frac{1}{s_{27}}-\frac{1}{2}\right), \tag{A3d}$$

$$R_5=(243r^3-318r^2-361r+340),$$

$$b_2=b_1/2, \tag{A3e}$$

$$b_3=b_4=b_5=r_2, \tag{A3f}$$

$$b_6=r_1, \tag{A3g}$$

$$r_1=\frac{8}{(12+a^2)}\left(\frac{1}{s_{27}}-\frac{1}{2}\right), \tag{A3h}$$

$$r_2=c_T^2\frac{R_6}{R_5}\left(\frac{1}{s_{27}}-\frac{1}{2}\right), \tag{A3i}$$

$$R_6=(3r+5)(12r^2-17r+17),$$

$$\omega_6=\frac{2}{3}\frac{(3r-2)}{(3r+1)}, \tag{A3j}$$

$$\omega_7=-\frac{(r-1)}{(r+3)}. \tag{A3k}$$

With the above formulas for c_1 and c_2, the parameter b^2 becomes

$$b^2=\frac{8a^2+3(3r+1)}{(1-r)}. \tag{A4}$$

Therefore, there are only four coupling coefficients that remain to be determined: a, a_2, a_3, and r. The ranges of these parameters will be determined by the positivities of b^2, c_s^2, c_T^2, and of the transport coefficients. In addition, the stability of the model must be tested by numerical computations of the eigenvalues of the dispersion equation for a wide range of values of k: this will help choose the relaxation parameters available (s_2, s_3, s_4, s_{15}, s_{19}, s_{27}, and s_{28}).

APPENDIX B: TRANSPORT COEFFICIENTS OF THE MODEL

There are twelve relaxation parameters in the model: s_2, s_3, s_4, s_6, s_7, s_r, s_{15}, s_{19}, s_{24}, s_{27}, s_{28}, and s_{30}. Isotropy criteria require that four of s_α's depend on others:

$$\tilde{s}_6=\omega_6\tilde{s}_{27}, \tag{B1a}$$

$$\tilde{s}_7=\omega_7\tilde{s}_{27}, \tag{B1b}$$

$$\tilde{s}_{24}=\frac{1}{4}\tilde{s}_{27}, \tag{B1c}$$

$$\tilde{s}_{28}=\frac{b^2}{6a^2}\tilde{s}_{30}, \tag{B1d}$$

where

$$\frac{1}{\tilde{s}_\alpha}\equiv\frac{1}{s_\alpha}-\frac{1}{2}. \tag{B2}$$

The speed of sound wave, c_s, transverse wave, c_T, and longitudinal wave, c_L, are

$$c_s^2=\frac{1}{72}(64+a_2), \tag{B3a}$$

$$c_T^2=\frac{3}{2}\frac{(4-3c_1-c_2)}{(12+a^2)}=\frac{144}{(12+a^2)}\frac{(r-1)R_5}{(21r-29)R_2}, \tag{B3b}$$

$$c_L^2=\frac{4}{3}c_T^2+c_s^2, \tag{B3c}$$

where the expressions for c_1 and c_2 have been substituted in c_T^2, and R_2 and R_5 are given in Eqs. (A3). The nonrelaxing shear and bulk viscosities of the model are

$$\tilde{\nu}_0=\frac{1}{12}a^2c_T^2\left(\frac{1}{s_{30}}-\frac{1}{2}\right), \tag{B4a}$$

$$\zeta_0=\frac{1}{72}(8+36c_1-a_2)\left(\frac{1}{s_2}-\frac{1}{2}\right). \tag{B4b}$$

Attenuation coefficients for transverse, longitudinal, and diffusive waves in the low frequency limit are:

$$\gamma_T^0=c_T^2\left[\left(\frac{1}{s_r}-\frac{1}{2}\right)+\frac{a^2}{12}\left(\frac{1}{s_{30}}-\frac{1}{2}\right)\right], \tag{B5a}$$

$$\gamma_L^0=\frac{1}{2}\zeta_0+\frac{2}{3}\gamma_T^0, \tag{B5b}$$

and in the high-frequency limit are

$$\gamma_T^\infty=\frac{1}{2}(r_1+3r_2)+\frac{1}{2}\tilde{\nu}_0, \tag{B6a}$$

$$\gamma_L^\infty=\frac{[2(r_1+4r_2)+b_1]c_T^2}{(3c_s^2+4c_T^2)}+\frac{1}{2}\tilde{\nu}_0+\frac{2}{3}\zeta_0, \tag{B6b}$$

$$\gamma_0^\infty=\frac{3(r_1+4r_2)c_s^2-2b_1c_T^2}{(3c_s^2+4c_T^2)}. \tag{B6c}$$

The diffusion coefficient is

$$D_0=\frac{8}{(12+a^2)}\left(\frac{1}{s_{27}}-\frac{1}{2}\right). \tag{B7}$$

[1] G. McNamara and G. Zanetti, Phys. Rev. Lett. **61**, 2332 (1988).
[2] F.J. Higuera, S. Succi, and R. Benzi, Europhys. Lett. **9**, 345 (1989).
[3] H. Chen, S. Chen, and W.H. Matthaeus, Phys. Rev. A **45**, R5339 (1992).
[4] Y.H. Qian, D. d'Humières, and P. Lallemand, Europhys. Lett. **17**, 479 (1992).
[5] R. Benzi, S. Succi, and M. Vergassola, Phys. Rep. **222**, 145 (1992).
[6] X. He and L.-S. Luo, Phys. Rev. E **55**, R6333 (1997).
[7] X. He and L.-S. Luo, Phys. Rev. E **56**, 6811 (1997).
[8] X. He and L.-S. Luo, J. Stat. Phys. **88**, 927 (1997).
[9] S. Chen and G.D. Doolen, Annu. Rev. Fluid Mech. **30**, 329 (1998).
[10] U. Frisch, B. Hasslacher, and Y. Pomeau, Phys. Rev. Lett. **56**, 1505 (1986).
[11] S. Wolfram, J. Stat. Phys. **45**, 471 (1986).
[12] U. Frisch, D. d'Humières, B. Hasslacher, P. Lallemand, Y. Pomeau, and J.-P. Rivet, Complex Syst. **1**, 649 (1987).
[13] D. d'Humières, Prog. Astronaut. Aeronaut. **159**, 450 (1992).
[14] L. Giraud, D. d'Humières, and P. Lallemand, Int. J. Mod. Phys. C **8**, 805 (1997).
[15] L. Giraud, D. d'Humières, and P. Lallemand, Europhys. Lett. **42**, 625 (1998).
[16] D. d'Humières and P. Lallemand, C. R. Acad. Sci. Paris, Série II **317**, 997 (1993).
[17] R.B. Bird, R.C. Armstrong, and O. Hassager, *Dynamics of Polymeric Liquids*, 2nd ed. (Wiley, New York, 1987), Vol. 1.
[18] P. Lallemand and L.-S. Luo, Phys. Rev. E **61**, 6546 (2000).
[19] L.-S. Luo, Ph.D. thesis, Georgia Institute of Technology, 1993 (unpublished).
[20] L.-S. Luo, J. Stat. Phys. **88**, 913 (1997).
[21] M. Hénon, Complex Syst. **1**, 762 (1987).
[22] Y. Qian and Y. Deng, Phys. Rev. Lett. **79**, 2742 (1997).
[23] I. Ispolatov and M. Grant, Phys. Rev. E **65**, 056704 (2002).
[24] K.F. Herzfeld and T.A. Litovitz, *Absorption and Dispersion of Ultrasonic Waves* (Academic, New York, 1959).
[25] L.-S. Luo, Comput. Phys. Commun. **129**, 63 (2000).
[26] F.R.W. McCourt, J.J.M. Beenakker, W.E. Kóhler, and I. Kuščer, *Nonequilibrium Phenomena in Polyatomic Gases* (Clarendon Press, Oxford, 1990), Vol. 1.
[27] P. Lallemand and L.-S. Luo (unpublished).
[28] P. L. Bhatnagar, E. P. Gross, and M. Krook, Phys. Rev. **94**, 511 (1954).